Quaternary Research (2023), **116**, 78–95
doi:10.1017/qua.2023.44

Research Article

Late glacial through Early Holocene environments inferred using pollen from coprolites and sediments recovered from Paisley Caves, Oregon

Chantel V. Saban[1]*, Erin M. Herring[1], Dennis L. Jenkins[2] and Daniel G. Gavin[1]

[1]Department of Geography, University of Oregon, Eugene, OR 97403, USA and [2]Museum of Natural and Cultural History, University of Oregon, Eugene, OR 97403, USA

Abstract

The Paisley Cave archeological site in the Northern Great Basin has provided a rich archaeological record from 13,000 to 6000 cal yr BP, including abundant mammalian coprolites preserved in a well-dated stratigraphy. Here we analyze and contrast pollen from within coprolites and pollen in associated sediments to examine vegetation history and assess whether coprolite pollen provides unique information with respect to the coprolite producer, such as the use of specific habitats, foods, or water sources. We found that the dissimilarity of pollen assemblages between coprolites and associated sediments was greater than the serial dissimilarity between stratigraphically adjacent samples within either group. Serial dissimilarity within types was not greater for coprolites than sediments, as would be expected if there were unique pollen signatures derived from the short period (1–2 days) represented by each coprolite. Compared with sediment pollen assemblages, the coprolites had higher abundances of lighter pollen types, and some individual samples were high in wetland taxa (especially *Typha*). Our results are consistent with coprolite pollen representing short time periods collected as a mammal moves on the landscape, whereas sediment pollen reflects longer time periods and more regional vegetation indicators.

Keywords: Pollen, Coprolite, Sediment, Caves, Paisley Caves, Northern Great Basin, North America, Late glacial, Early Holocene, Fire regimens, Ordination, NMDS

(Received 19 October 2022; accepted 26 July 2023)

INTRODUCTION

The postglacial vegetation history of the Northern Great Basin (NGB) has been strongly affected by the balance of moisture from the Pacific Ocean and continental dry and warm air masses moving north from the Central Great Basin (Wigand and Rhode, 2002; Minckley et al., 2007). Although large lakes persisted in the basins of the NGB through the late Pleistocene, decreased effective moisture and increased evapotranspiration since 11,000 cal yr BP have resulted in the desiccation of these pluvial lakes and subsequent deflation of Pleistocene sediments, generally precluding the use of these larger basins as reliable archives of postglacial climate change (Allison, 1982; Cohen et al., 2000). Understanding postglacial environments and reconstructing the heterogeneity of this landscape has implications for understanding the environments experienced by humans and other animals, which is especially important, as the NGB has evidence of some of the oldest human activity in North America (Gilbert et al., 2008; Jenkins et al., 2012; McDonough, 2019), as well as extinct and extant megafauna remains (McDonough et al., 2012; Jenkins et al., 2013).

Many postglacial pollen records recovered from within the NGB have been studied at mid- to high-elevation sites, as low-elevation sites containing undisturbed sedimentary sequences that span the Holocene are uncommon (Cohen et al., 2000). The few low-elevation pollen records that do exist reveal the ubiquitous presence of xeric shrub–steppe vegetation since the last glacial maximum (Mehringer, 1987; Wigand, 1987; Wigand and Rhode, 2002; Mensing et al., 2013; Beck et al., 2018; Kennedy, 2018; McDonough et al., 2022). However, wetlands are embedded within this xeric landscape. In various places, drainages from mountains feed into seasonal or persistent wetlands, resulting in a sharp contrast between wet and xeric plant communities, as hydrophytic plants respond rapidly to changes in water availability (Kovalchik and Chitwood, 1990; Nowak et al., 1994).

Terrestrial caves often serve as natural subaerial sediment traps and can preserve organic materials for thousands of years (White, 2007). Archaeological investigations of caves and rock shelters occasionally yield preserved mammalian coprolites, offering opportunities to gain information about the diet and health of animals and to make inferences about past climates and environments (Bryant, 1974; Hofreiter et al., 2000; Carrión et al., 2001; Gilbert et al., 2008; Riley, 2008; Shillito et al., 2011; Wood and Wilmshurst, 2012, 2016; Beck et al., 2018, 2020; Blong et al., 2020). Coprolite studies have been an important component of Great Basin archaeological research since the early twentieth century (Loud and Harrington, 1929; Heizer, 1969; Heizer et al., 1970; Kelso, 1971; Thomas et al., 1983) and have since greatly expanded our understanding of past human behaviors and health (Jenkins et al., 2012, 2013; Dexter and Saban, 2014; Beck et al.,

*Corresponding author: Chantel V. Saban; Email: csaban@uoregon.edu

Cite this article: Saban CV, Herring EM, Jenkins DL, Gavin DG (2023). Late glacial through Early Holocene environments inferred using pollen from coprolites and sediments recovered from Paisley Caves, Oregon. *Quaternary Research* **116**, 78–95. https://doi.org/10.1017/qua.2023.44

2018; Kennedy, 2018; McDonough, 2019; Blong et al., 2020; McDonough et al., 2022).

Located in south-central Oregon within the NGB, the Paisley 5-Mile Point archaeological site (Paisley Caves) produced a material assemblage that includes abundant coprolites, providing opportunities for expanding the interpretation of pollen records from cave sediments. More than 2800 mammalian coprolites were excavated from Paisley Caves between 2002 and 2011 (Jenkins et al., 2012, 2013), and each represents a point in time during the last 14,300 yr. In this study, we assess the environmental conditions present during periods of wetland expansion and subsequent lake retreat in the Summer Lake basin between 14,000 and 6000 cal yr BP by comparing pollen assemblages of coprolites and their associated sediments. With this approach, pollen recovered from sediments represents multidecadal periods of sedimentation, while coprolite pollen offers a different view of environmental conditions due to a short (several-day) "sampling" period. The Paisley Caves are situated in close proximity to three ecotones: lacustrine–wetland, sagebrush steppe, and conifer forest (Cronquist et al., 1972; Franklin and Dyrness, 1988; Anderson et al., 1998). Contrasting pollen assemblages of sediments and coprolites may help clarify the paleovegetation history, which is still not well understood at low-elevation NGB sites.

Five previous studies of pollen and macrobotanical assemblages were conducted at Paisley Caves. First, Saban (2015) produced a pollen record from the same sampling unit (Cave 2, Unit 6B) as this study and is succeeded by the present study. Second, Beck et al. (2018) produced a pollen record from the same cave as this study (Cave 2), but located 1 m north of our sampled profile at a site with a different chronology and potentially different taphonomic processes (e.g., exposure to wind). Third, Kennedy (2018) identified macrobotanical remains from Cave 2 and developed a detailed description of local vegetation and cultural foods and plant resources. Fourth, Beck et al. (2020), at the same profile as Beck et al. (2018), compared *Neotoma* spp. (packrat) coprolite pollen assemblages with sediment pollen assemblages. Due to the small mass of *Neotoma* coprolites, Beck et al. (2020) merged 57 coprolites into single samples resulting in a total of fifteen 0.25 g samples of packrat coprolites. Pollen assemblages of *Neotoma* coprolites were statistically very similar to those in associated sediments, but coprolite pollen assemblages were more variable than those from sediments, possibly due to meal choice (Beck et al., 2020). Finally, Blong et al. (2020) examined contents of nine coprolites identified as originating from humans from the Younger Dryas (YD) through the Early Holocene for the purpose of reconstructing prehistoric human diets. That study found seeds, bones of small mammal and fish, and beetle remains in the coprolites, supporting foraging in marshes. Blong et al. (2020) also conducted limited pollen analyses, which found elevated percentages of insect-pollenated taxa and pollen aggregates, suggesting direct consumption of pollen.

DNA analysis of other coprolites from Paisley Caves have revealed coprolites associated with *Homo sapiens*, Camelidae, *Lynx*, *Ovis*, and *Panthera* (Jenkins et al., 2012). In addition to preserving the oldest human coprolites in North America, the Paisley Caves boast an extensive assortment of organic artifacts and materials that offer invaluable insights into the activities of humans and fauna from more than 14,000 yr ago. However, our comprehension of how humans and large mammals traversed the ancient landscapes of the NGB remains limited. Given the limited past analyses of mammalian coprolite pollen at Paisley Caves (Blong et al., 2020), there remains a potential for this approach to provide us with a better understanding of how large mammals roamed the local environment and left behind evidence of their movements at the caves.

Traditionally, mammalian coprolite analysis from archaeological sites in North America has been used to reconstruct diet, health (Bryant and Holloway, 1983; Bryant and Reinhard, 2012; Blong et al., 2020), and human activities at a site (Gilbert et al., 2008; Jenkins et al., 2012; McDonough, 2019; Shillito et al., 2020). This study uses coprolite pollen solely as an environmental proxy to reconstruct conditions at and beyond the caves. Pollen found in coprolites represents short periods of time, approximately 19–37 hours (Kelso and Solomon, 2006), and is derived from various sources: pollen in drinking water, airborne pollen that entered nasal and esophageal mucus, pollen adhered to any food item, pollen in ingested flowers or pollen cones, or pollen in the stomach content of prey (Carrión et al., 2001; Chame, 2003). Thus, coprolite pollen represents a brief period that can potentially reveal different information than sediment pollen. This study is unique in using coprolites as distinct pollen samples for direct statistical comparison to contemporaneous sediments and considering all taphonomic pathways (not only diet) behind the formation of the coprolite pollen assemblage (Shillito et al., 2020).

Interpretation of pollen assemblages from cave sediments can be limited for several reasons. Caves often contain both eolian and slopewash sediment, filtered from the environment via the single depositional entry of the cave opening. Also, within the NGB, redeposition of sediments blown off dry lakebeds may contribute pollen from prior climatic periods (Anderson, 1955). The location of the sediment samples relative to the layout of the cave may affect pollen assemblages due to, for example, pollen degradation caused by temperature exposure or physical degradation within a drip zone. Finally, bioturbation of sediments by faunal or human activities can disturb or erase the chronological integrity of sedimentary sequences, resulting in time-averaged pollen assemblages.

We hypothesize that differences in the pollen assemblages between cave sediment and coprolites emerge primarily due to the unique sampling of the environment by a mammal. We therefore predict that (1) pollen assemblages will differ more between coprolites and associated sediments than between samples within either group; (2) pollen assemblage turnover (i.e., rate of change) will be greater for coprolites than in sediments due to the potentially stochastic processes that determine the coprolite pollen assemblage; and (3) pollen taxonomic diversity will be greater in sediments than in coprolites, as sediments sample a larger spatial and temporal window of pollen deposition than do coprolites.

STUDY AREA

Geologic setting

Summer Lake basin is located within the larger Chewaucan Basin, a V-shaped graben delineated by steep fault scarps and subdivided into three subbasins: Summer Lake lies in the northwest portion of the V, with the basin that holds Upper and Lower Chewaucan Marshes in the south, and Lake Abert in the northeast (Fig. 1). The Chewaucan Basin graben dips northwest, with the Summer Lake basin floor averaging 1275 m above sea level (m asl), Upper and Lower Chewaucan Marshes averaging 1314 m, and the Lake Abert basin averaging 1299 m asl.

https://doi.org/10.1017/qua.2023.44 Published online by Cambridge University Press

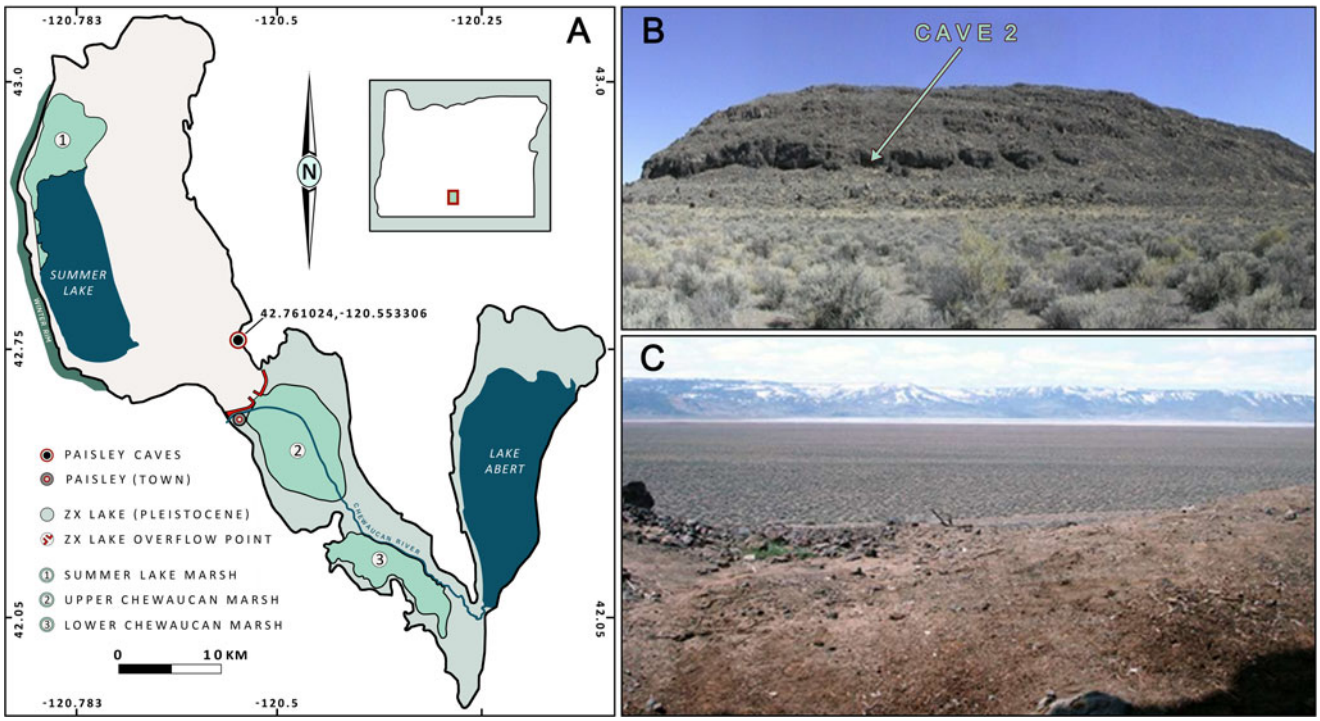

Figure 1. (**A**) Location of 5-Mile Point Butte and Paisley Caves in the Chewaucan Basin of south-central Oregon. Black line shows the maximum high-water extent of pluvial lakes during the late Pleistocene. (**B**) View of 5-Mile Point Butte, facing east. (**C**) View of Winter Rim from Cave 5, Paisley Caves, facing west.

The Paisley Caves are located on 5-Mile Point Butte, a scoriaceous basalt fault block butte located in the southeastern part of Summer Lake basin in south-central Oregon. This site is approximately 18 km east of the current Summer Lake shoreline and 8 km north of the Chewaucan River (Fig. 1). The caves are all on a southwest aspect, and their entrances are located midway up the butte at an average elevation of 1366 m asl (Fig. 1B). A series of eight wave-cut caves and rock shelters formed as a result of energetic wave action by Lake Chewaucan during periods of stable high lake stands (Allison, 1982; Friedel, 1993; Jenkins et al., 2013). Subsequent rockfalls at cave entrances have since resulted in some of the deeper caves developing into shallow rock shelters.

The current dry lakebed near 5-Mile Point Butte dips west at a 3.3° slope until the lakebed abruptly ends at the base of Winter Rim. The topography of the area north of 5-Mile Point Butte is characterized by dry lake flats, deflated playas, lunettes, and dune systems, with some small basalt fault block outcrops. East of 5-Mile Point Butte the topography rises in elevation above the lakebed floor and is less steep than the west side of Summer Lake basin. This east side is composed of fault block features that increase in elevation for 13 km up to approximately 1590 m, after which the topography then slopes down 13 km east to Lake Abert. The Summer Lake lakebed slopes little south of 5-Mile Point Butte, where the topography is interrupted by the incised course of a stream that resulted from the overflow of ZX Lake into Summer Lake during the YD (Allison, 1982; Friedel, 1993; Licciardi, 2001; Hudson et al., 2021).

Pluvial Lake Chewaucan covered an area of 1243 km^2 at its maximum extent, with a surface elevation of 1381 m asl and a maximum depth of ca. 118 m (Allison, 1982; Cohen et al., 2000). The primary stream feeding Lake Chewaucan was the Chewaucan River, draining north through a steep river valley into the Chewaucan Basin. During the late Pleistocene Bølling-Allerød (BA) period, 14,700 to 12,900 cal yr BP (Sowers and Bender, 1995), water levels in Lake Chewaucan reached their last high stand by ca.14,500 cal yr BP, after which levels declined and Chewaucan River sediments formed the Paisley Fan (1323 m asl) at the south end of Summer Lake, resulting in Summer Lake hydrologically separating from the rest of the Chewaucan basin (Allison, 1982; Licciardi, 2001). Basal sediments in this current study were dated to ca. 14,000 cal yr BP, the time of the Chewaucan high stand.

The YD cold period (12,800–11,600 cal yr BP) is characterized by a return to cooler temperatures in the Northern Hemisphere (Mayewski et al., 1993; Rasmussen et al., 2014). At this time, Summer Lake began receding due to lower precipitation and increasing summer insolation (Hudson et al., 2019, 2021). The climate began to warm after the YD, eventually resulting in climatic conditions being warmer during the earliest portions of the Holocene (11,000–9000 cal yr BP), with evidence of a brief period of increased precipitation that resulted in a transgression of Summer Lake to moderately high levels, although not as high as during the BA (Hudson et al., 2021). Conditions reached thermal and aridity maxima after 9000 cal yr BP, after which climatic conditions began to cool but remained arid (Friedel, 1993; Bartlein et al., 1998, 2011; Cohen et al., 2000; Benson et al., 2002; Mensing et al., 2004; Minckley et al., 2007; Long et al., 2019; Hudson et al., 2021).

Climate and vegetation

The Summer Lake basin is presently located at a convergence zone of moist Pacific air parcels moving inland from the southwest and continental climate characterized by a high-pressure system centered above the Central Great Basin in Nevada to the

https://doi.org/10.1017/qua.2023.44 Published online by Cambridge University Press

southeast of the Chewaucan Basin, which have varied over the Holocene (Reinemann et al., 2009; Carter et al., 2017; Long et al., 2019). Geographically located in the rain shadow of the Cascade Range, the NGB region currently has warm summers and cold winters (mean July and January temperatures 17.7°C and 2.2°C, respectively). Average annual precipitation is 33.9 cm; most precipitation occurs from November through January, with afternoon thunderstorms during summer seasons.

Vegetation gradients in the region are primarily determined by elevation and its effects on orographic precipitation (Franklin and Dyrness, 1988; Kovalchik and Chitwood, 1990; Osmond et al., 1990). Current Summer Lake basin vegetation is high desert shrub–steppe dominated by *Artemisia tridentata* and salt-tolerant Amaranthaceae (*Chenopodium* and *Atriplex*; Franklin and Dyrness, 1988; St. Louis, 2021). The *A. tridentata* community includes an understory of the invasive *Bromus tectorum*, as well as *Elymus* sp., *Ericameria teretifolia*, *Sarcobatus vermiculatus*, and various other shrubs, forbs, and grasses adapted to sandy eolian sediments and highly alkaline aridisols. At the base of 5-Mile Point Butte, the lakebed sharply transitions into a steep, rocky talus of basalt boulders with pockets of playa loess accumulating between the boulder gaps. Vegetation on the talus slope is primarily *Artemisia* and *Chrysothamnus* sp. with intermittent cespitose *Eriogonum* sp. and hemiparasitic *Castilleja angustifolia*.

The trees currently nearest to the caves are 8 km to the south at the town of Paisley, where riparian vegetation extends along the Chewaucan River into Upper Chewaucan Marsh. Modern-day trees and shrubs include *Pinus ponderosa*, *Alnus incana*, *Betula occidentalis*, *Juniperus occidentalis*, *Prunus virginiana*, *Salix* sp., *Populus tremuloides*, *Populus trichocarpa*, and non-native *Populus alba*. A very small population of *Quercus garryana* var. *semota* was reported on Gearhart Mountain at 1650 m asl (https://oregonflora.org/taxa/index.php?taxon=14318). Nonnative *Medicago sativa* is grown in center-pivot irrigation fields within a few kilometers of the caves. Marsh plants are present in both the Upper and Lower Chewaucan Marshes, near the Summer Lake Hot Springs ca. 8 km west of 5-Mile Point Butte, along most of the 40 km base of Winter Rim, and at the north end of the Summer Lake basin at the Summer Lake Wildlife Area 24 km north of 5-Mile Point Butte. The marsh communities include a range of Poaceae, Juncaceae, Cyperaceae, *Ribes* sp., Typhaceae, and Asteraceae. Trees present 20 km west of 5-Mile Point Butte on the steep scarp of Winter Rim (2200 m elevation) include *P. trichocarpa* and *P. alba*, *P. virginiana* at the base; *P. ponderosa*, *Salix* sp., *J. occidentalis*, *P. tremuloides* at mid-elevation; and *Pinus contorta* and *Abies concolor* at the Winter Rim summit.

Archaeological excavations at Paisley Caves

Sediments and coprolites used in this study were all collected during archaeological research at Paisley Caves between 2009 and 2011. Archaeological research began in 1938 under University of Oregon archaeologist Luther S. Cressman (Cressman, 1940; Jenkins et al., 2004), who numbered the caves sequentially from south to north. From 2002 to 2011, DLJ directed further excavations at the site for the University of Oregon. Materials recovered ranged from artifacts such as lithic tools and debitage, bone, antler, and wood tools, cordage, and grinding stones (manos and metates), as well as a rich array of organic materials that included plant macrofossils; insects; the bones of fish, waterfowl, small mammals, extant and extinct megafauna, and reptiles; and 2533 coprolites of human and other mammalian origins. Gilbert et al. (2008) reported on the DNA sequencing of three ca. 14,000-yr-old human coprolites, which at the time of publication were the oldest confirmed human remains in the Western Hemisphere.

Materials dated to the YD period showed human activity was very high in Paisley Cave 2, with cultural material deposits becoming dense enough to create a culturally formed stratigraphic level referred to as the Botanical Lens (BL). BL deposits are composed primarily of a 5- to 8-cm-thick mat of *Artemisia* twigs and shredded bark and contained a hearth dated to the YD (Jenkins et al., 2013). The BL is underlain by a 1–3 cm alluvial mud lens dated to ca. 12,930 cal yr BP and capped by a second 1–2 cm mud lens dated to ca. 11,500 cal yr BP.

The coprolites and sediments used in this study were excavated from Cave 2, Unit 2/6 (Fig. 2). Materials from this unit were selected for this project due to the high number of well-mapped, stratigraphically sequential, and large mammalian coprolites with associated sediments, as well as for the minimal westward slope of the cave floor (Fig. 3). Cave 2 is approximately 7 m long, 6 m wide, and 3 m deep; 30.3 m^3 of sediment over 22 m^2 has been excavated from this cave (Jenkins et al., 2013). The cave walls are composed of fine-grained basalts mixed with soft volcanic tuffs and breccias. Summer Lake basin is a seismically active area (Licciardi, 2001; Badger and Watters, 2004; Orr and Orr, 2012) resulting in roof falls being common in the caves. Roof fall materials range from small pebbles to multi-ton boulders, the most notable of which was once the outer ceiling of Cave 2, which now blocks most of the entrance to the cave. The age of the roof fall is ca. 2,300 cal yr BP based on a radiocarbon date obtained from a human coprolite recovered from beneath a smaller boulder from the same event (Jenkins et al., 2013). In 1939, Luther Cressman excavated a trench in Cave 2 but missed unit 2/6 due to the presence of the roof-fall boulders. Looters who later dug up the Cressman trench also missed the 2/6 sediments for the same reason. The larger boulder remains in place, but the smaller one was removed in 2009. Cave 2 was divided into seven 2 m × 2 m plots that were further subdivided into 1 m × 1 m units (Fig. 2). By the end of Cave 2 excavations in 2011, the cave had been excavated in primarily 5 cm increments down to bedrock at a depth of ca. 308 cm.

Sediment description

Cave 2 sediments are composed of both biological and exogenetic materials (Jenkins et al., 2012) and include varying amounts of eolian deposits, rockfall, bat guano, rodent feces, deposited cultural materials, and vegetation blown in or brought into the rock shelter by *Neotoma* sp. Areas under smaller rockfall boulders not excavated by Cressman in 1938 were bioturbated by rodents or badgers or destroyed by looters in places, but overall the sediment matrices were well preserved and in excellent sequential order (Jenkins et al., 2012). This was largely due to millennia of urine accumulation forming hydrophobic and waterproof indurated sediments (Jenkins et al., 2012). A cross-section of the remaining 2/6 west sediment wall (Fig. 3) shows the stratigraphy before excavations. Cave 2 has an average sedimentation rate of approximately 50 yr/cm, with the exception of the BL, which is primarily of anthropogenic origin, and the 30 cm of Mazama tephra representing a single event (Jenkins et al., 2016).

Lithostratigraphic units (LUs) are distinct sediment types that make up the matrices of sedimentary units and are defined by

https://doi.org/10.1017/qua.2023.44 Published online by Cambridge University Press

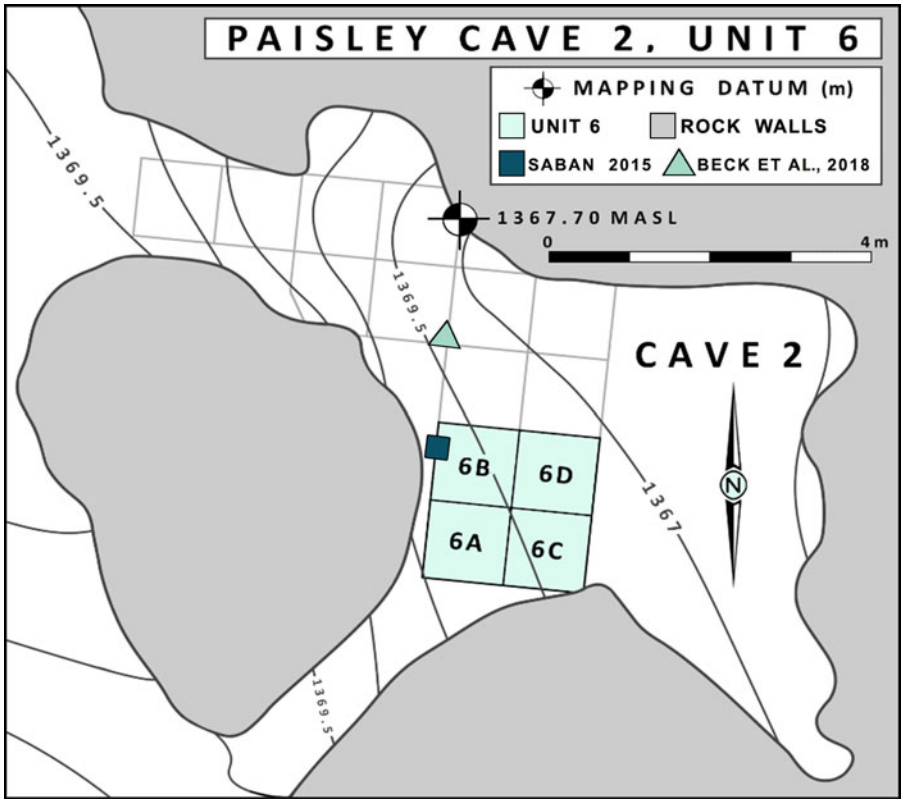

Figure 2. Cave 2 showing location of Unit 6 relative to datum and roof-fall boulder at west end of entrance. Previous sediment sampling by Saban (2015) shown as small teal box and Beck et al. (2018) sampling shown as small green triangle. Map image redrawn from Jenkins et al. (2012).

their sediment characteristics (Gasche and Tunca, 1983; Stein, 1987). Seven LUs were identified in Cave 2 (Fig. 3), although only three are relevant here. LU1 overlays basement rock in a portion of 2/6B that was not sampled for this project. LU2 is a dark-brown, poorly sorted gravelly sand approximately 30 cm thick overlying basement rock or LU1. A distinct transition from LU2 to LU3 occurs at ca. 260 cm and has been dated to 12,500 cal yr BP. The transition is marked by a patchy occurrence of the BL (described earlier) and includes a small hearth of charred organic material overlain by ashy/organic sediment. LU3 extends up to the cataclysmic eruption of Mount Mazama 7633 cal yr BP (Egan 2015). LU3 is a mix of fine eolian-deposited sediments, some smaller poorly sorted gravels mixed with angular roof fall, and heavy organic components of plant materials and bat guano (Jenkins et al., 2012). LU3 sediments are firm to hard, of polygenetic origins with abundant macrobotanical content, amorphous organic matter, and high amounts of *Neotoma* and *Chiroptera* feces (Jenkins et al., 2012). Weakly consolidated Mazama tephra (152–180 cm) was assigned as LU4. Guano pellets from the base of the Mazama tephra were dated to 7633 cal yr BP (Jenkins et al., 2013). Laminations and fine ash capping and underlying the tephra suggests primary tephra deposition at the west end of Unit 2/6 (Fig. 3). The tephra in the 2/6 west wall ranges from fine ash to pale yellow rhyolitic lapilli from 1 to 1.5 mm in size. The topmost sediments for this unit are referred to as LU5 and contained little to no Mazama tephra (Jenkins et al., 2012).

MATERIAL AND METHODS

Material collection during excavations

All coprolites found in situ during excavations in Cave 2 from 2009 to 2011 were collected following strict protocols to limit their exposure to modern-day DNA contamination. These collection protocols included Tyvek hazmat suits, sterile gloves, forceps, and specimen cups. For most of the sampled coprolites, a sediment sample was also taken directly below the coprolite. Both samples were then sealed into sterile specimen cups and labeled. All coprolites selected for the study had an associated sample of sedimentary materials collected at the same time. No effort was made to distinguish human coprolites from those of other large carnivorous or omnivorous mammals. The coprolites were desiccated and ranged from very light tan to medium brown (Fig. 4). Faunal fragment analysis resulted in 6 to 20 bone fragments per coprolite sample, ranging from 3 to 8 mm in size, and included mammalian and avian bone fragments (Cromwell, R.P., personal communication, 2016). All the bones were fragmented except for one rodent left tarsal, several rodent molars, the dentin sheath of a rodent incisor, and two rodent claws. Positions of artifacts and radiocarbon dates were changed from elevation (m) to centimeters below the modern cave floor (1368.3 m) for subsequent analyses. All samples in this study are from unit 6B (Fig. 2). In this portion of the cave, undisturbed sediments were excavated at depths of 120 to 320 cm below the 1368.3 m asl elevation.

Lab processing

Coprolites

Sampling and chemical processing of both coprolites and sediments was conducted at the University of Oregon, where strict sampling procedures were followed to protect the remaining materials from modern DNA contamination. Coprolites were subsampled for pollen following methods outlined by Wood and Wilmshurst (2012, 2016), except for sectioning the coprolites along a longitudinal axis rather than the center. An average dry

https://doi.org/10.1017/qua.2023.44 Published online by Cambridge University Press

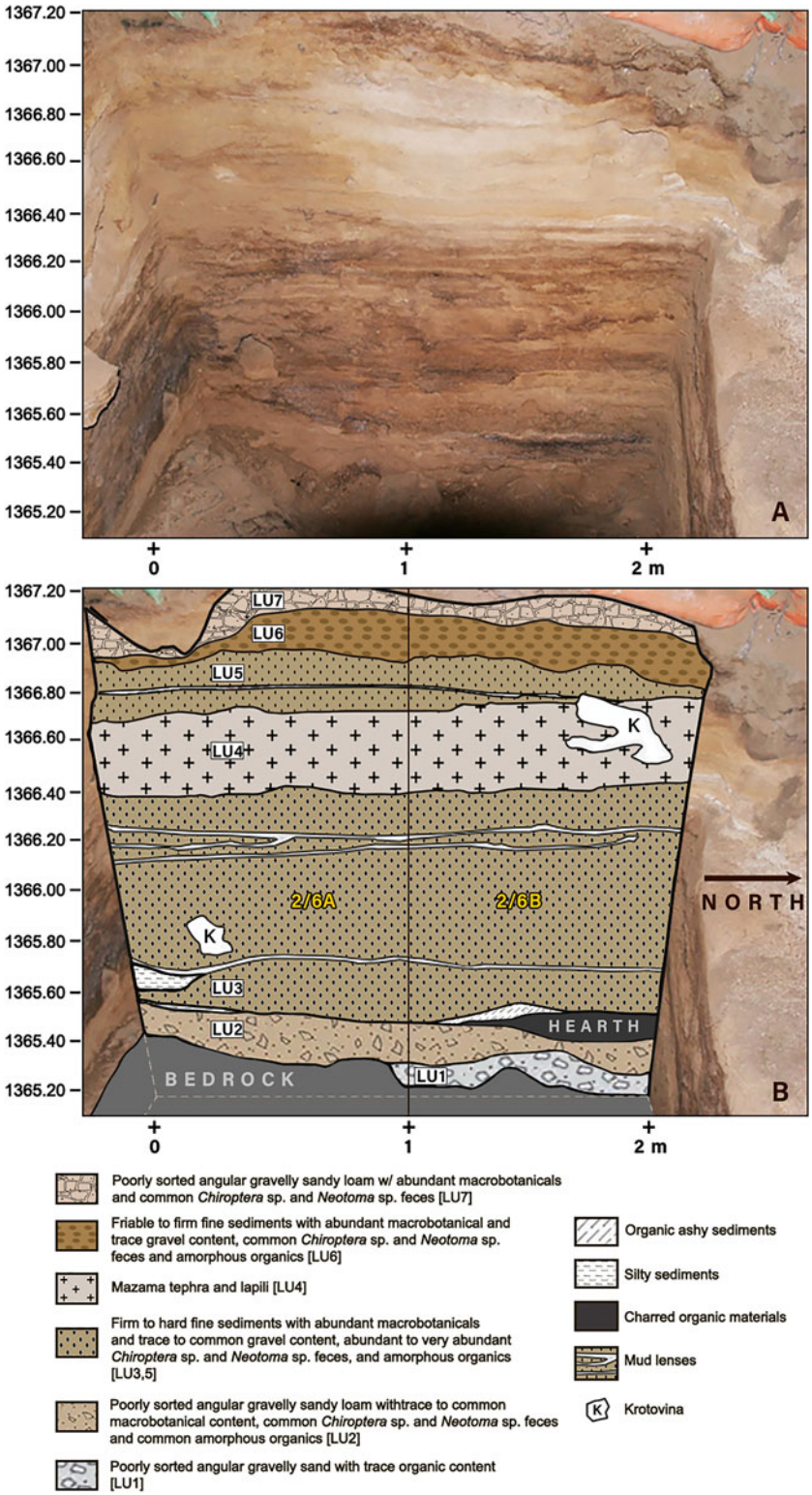

Figure 3. Remaining west wall of unit 2/6. This sediment wall is overlain by the roof collapse that occurred ~2000 cal yr BP. Visible in the photo are the tephra layer; indurated laminations; the remains of a small hearth, which is part of the BL; and rodent holes (krotovina). Bottom image and description were redrawn from Jenkins et al. (2012).

weight of 1.6 g (ranging from 0.668 to 3.638 g) was sampled from the center of each coprolite (Fig. 4). Coprolites lighter than 0.50 g were not processed.

The chemical process for pollen recovery from coprolites followed Pearsall (2016) and Smith (1998) but was modified to protect materials, including bone and plant fibers, for possible future radiocarbon dating. Chemical pollen extraction was performed inside a fume hood. Each coprolite subsample was placed in a 50 mL tube and spiked with one *Lycopodium* tablet to determine pollen concentration. Samples were rehydrated with 50 mL warm 10% sodium hexametaphosphate ($Na_6[(PO_3)_6]$) for 48–72 hours. Samples were sieved at 180 µm, and macrofossils were collected.

https://doi.org/10.1017/qua.2023.44 Published online by Cambridge University Press

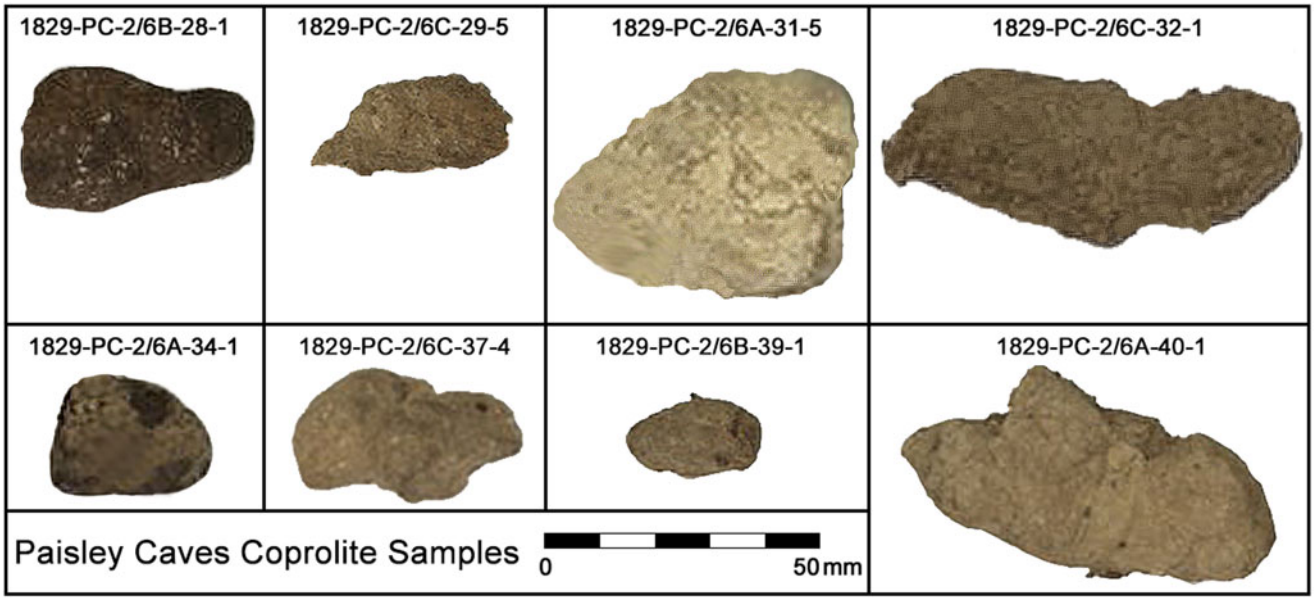

Figure 4. Examples of coprolite specimens used in this study. Colors range from light tan to dark brown. Photographs were taken in 2016.

Samples were treated with a 10% potassium hydroxide (KOH) at 80°C for 10 minutes, acetolysis (9:1 acetic anhydride:sulfuric acid, heated for 3 minutes). Samples were stained with Safranin and desiccated using ethyl alcohol and tert-butyl alcohol. Pollen was transferred into 2-dram glass vials with silicone oil used for suspension and preservation of pollen (Faegri et al., 1989).

Cave sediment

Pollen recovery from the Paisley sediments required some minor adjustments to the chemical extraction process from Smith (1998) and Pearsall (2016). Sediments were wet sieved using a 125 µm mesh until 20 cm^3 of the fine fraction was obtained. Each sample was added to a 1000 mL Nalgene beaker (12 samples per lab session) and spiked with one *Lycopodium* tablet to measure pollen concentrations. Samples were soaked in warm 10% $Na_6[(PO_3)_6]$. Sediments were agitated and allowed to settle for 8 hours, after which the water was partially decanted and replaced with distilled water (no additional $Na_6[(PO_3)_6]$ added), agitated, and allowed to settle for another 8 hours. This process was repeated for approximately 10–12 days until the water was clear. Then, 10% KOH (80°C, 10 minutes) was used to remove remaining soluble organics followed by a 10% hydrochloric acid (HCl) treatment to remove carbonate minerals. A cold hydrofluoric acid (HF) treatment for 24 hours reduced silicate content. Prior work on Cave 2 sediments showed that a cold HF treatment was more effective at removing silicates than a 45 minute hot HF treatment (Saban, 2015). Following a second 10% HCl treatment, the samples were rinsed with ultrapure water.

Following the Smith (1998) protocols for processing dry sediments, a heavy liquid solution (1.9–2.0 specific gravity) of zinc bromide ($ZnBr_2$) was used to separate pollen from heavier materials. Following centrifuging, pollen suspended on the heavy liquid was decanted into 50 mL centrifuge tubes. $ZnBr_2$ heavy liquid suspension was repeated twice per sample. The remaining sediments in their original centrifuge tubes were filled with ultrapure water, capped, and placed into storage boxes for possible future pollen recovery. The pollen fractions were diluted with water and centrifuged to remove the remaining $ZnBr_2$. Pollen was then transferred into 15 mL centrifuge tubes. Glacial acetic acid was used to remove water, followed by acetolysis (as for the coprolite samples) to remove the remaining cellulose. Samples were stained, desiccated, and suspended in silicone oil as described for the coprolite pollen.

Identifications

Pollen from both coprolites and sediments were examined at 400× magnification. Pollen was identified to the highest taxonomic resolution possible using published keys (Faegri et al., 1989) and the modern pollen reference collection at the University of Oregon. Both coprolite and sediment slides were counted to a minimum of 350 grains per sample, except for one coprolite with low pollen abundance, where only 175 pollen grains could be identified.

Chronology

An age–depth model was constructed using the INTCAL20 calibration curve and the Bacon R package (Blaauw and Christen, 2011; Reimer et al., 2020). The model is based on 16 radiocarbon dates available from unit 2/6 (Saban, 2015; Jenkins et al., 2016). We also obtained a new date on an unidentified plant macrofossil from a coprolite occurring above the Mazama tephra. A date of 7633 cal yr BP for the Mount Mazama eruption (Egan et al., 2015) was included in the age–depth model. In the Bacon model, we specified the Mazama tephra unit as an instantaneous event and placed a hiatus at 296.5 cm, where an abrupt change in ages corresponds roughly to the depth of the BL.

Statistical analyses

Raw pollen counts were transformed into percentages and diagramed using Tilia 3.0.1. Pollen assemblage zones of the sediment pollen record were determined using stratigraphically constrained cluster analysis. We used the rioja package in R statistical software

https://doi.org/10.1017/qua.2023.44 Published online by Cambridge University Press

to identify zones based upon the chord distance, calculated as the Euclidean distance of square-root-transformed pollen proportions. The number of significant pollen zones was determined using the broken stick method (Bennett, 1996).

Nonmetric multidimensional scaling (NMDS) gradient analysis was used to compare sediment and coprolite assemblage relationships. NMDS is an indirect gradient ordination analysis using a dissimilarity matrix that describes a pairwise difference between taxa assemblages. Pollen assemblage dissimilarity was measured with the chord distance using the *vegdist* and *metaMDS* functions in the vegan package in R (Oksanen et al., 2020). Both coprolites and sediments were included in the ordination, using the 29 taxa found in three or more samples.

Chord-distance dissimilarity was summarized between coprolites and adjacent sediment and between adjacent sediment and coprolite samples as a measure of stratigraphic turnover. Pollen taxa richness of coprolite and sediment samples was estimated with rarefaction for a sample of 175 pollen grains, using the *rarefy* function in vegan. The difference of rarefied pollen richness between coprolites and corresponding sediment samples was tested using a paired *t*-test.

RESULTS

Sediment age–depth model and pollen assemblage zones

Thirteen of the 17 radiocarbon ages occur in the lower 40 cm, surrounding the BL, and several were out of stratigraphic order. The Bacon age–depth model provides a best estimate of ages through periods of overlapping radiocarbon dates at the base of the section and also interpolates between ages at the top of the section (Fig. 5, Table 1). The basal age at 308 cm was modeled to 13,900 cal yr BP. Very slow accumulation occurred from 300 to 296 cm (encompassing 700 yr). Furthermore, a hiatus was required to fit the age model to a step change in the radiocarbon dates at 296.5 cm (12,700 to 12,200 cal yr BP), which corresponds to the BL between units LU2 and LU3. This hiatus does not appear to be present in other portions of Paisley Cave 2 (Beck et al. 2018). Instead of containing sediments, the BL is composed of organic materials, including artifacts, macrobotanicals, and coprolites. There were coprolites available from the BL, but as there were no corresponding sediments, they were not used in this study. Above this hiatus, fewer ages constrain the age model, but they show a generally fast sedimentation rate (20 yr/cm) that declined upward to the Mazama tephra (70 yr/cm).

Overall, pollen preservation was very good, with only <2% being indeterminable. The coprolites did not contain pollen aggregates, which have been interpreted as pollen being consumed directly (e.g., Blong et al., 2020). The stratigraphically constrained cluster analysis identified three zones in the sediment record, with breaks at 252 cm (11,100 cal yr BP) and 172 cm (within the Mazama-enriched sediment). The break at 252 cm corresponds roughly with the LU2/LU3 boundary. Pollen concentrations were sufficient for pollen analysis in the Mazama-enriched zone (LU4, 180–152 cm).

Sediment pollen record

P1: Late Pleistocene BA to Early Holocene

Period P1 covers a 2700-yr time span from 13,900 cal yr BP during the BA warm period, and following a sediment hiatus, to the Early Holocene (11,100 cal yr BP). A total of 20 taxa were identified (Fig. 6A). Common pollen types during P1 included *Pinus* subg. *Pinus* (increasing from 25% to 45%, then returning to 30%), *Pinus* subg. *Strobus* (1–2%), *Abies* (3–6%), *Pseudotsuga* (1–2%), *Acer* (1–2%), Betulaceae (1%), *Salix* (4–10%), Grossulariaceae (1%), Rhamnaceae (1%), *Artemisia* (15–28%), *Ambrosia*-type (11%, decreasing to 1%), Asteroideae-type (1%), Amaranthaceae (5%, increasing to 30%), Fabaceae (3–5%), Polygonaceae (3%), Onagraceae (1%), Typhaceae (3–4%), Alismastaceae (1%), and Poaceae (4%). Pollen concentrations declined from 120,000 grains/cm^3 in the sample before the hiatus to 50,000 grains/cm^3 after the hiatus, then increased to 80,000 grains/cm^3.

P2a: Early Holocene to the Mazama tephra

P2a ranges from the Early Holocene at 11,100 cal yr BP to the Mazama tephra at 7633 cal yr BP. Thirty taxa were identified. *Abies* increased sharply from 7% to 21% at the start of P2a and remained at approximately 20% until the Mazama tephra. During this time, *Artemisia* declined from 24% to 10%. *Pinus* subg. *Pinus* pollen remained consistently between 28 and 35%, and *Pinus* subg. *Strobus* declined to below 1%. Conifers also included *Picea* (0–4%) and *Pseudotsuga* (1%). Other taxa included Taxaceae (1–2%), Cupressaceae (1–2%), Betulaceae (1–5%), *Alnus* undiff. (1–2%), *Salix* (1–5%), *Populus* undiff. (1–3%), Aceraceae (3%), Celestraceae (1%), *Artemisia* (9–20%), Asteroideae-type (1–5%), *Ambrosia*-type (1–4%), Amaranthaceae (8–23%), Brassicaceae (1–7%), Fabaceae (2–5%), Onagraceae (1–2%), Solanaceae (1%), Typhaceae (1–4%), Cyperaceae (0–4%), and Poaceae (2–7%). Pollen concentrations were generally high (>90,000 grains/cm^3) before the Mazama unit and were lower (21,000–60,000 grains/cm^3) within the Mazama unit.

P2b: Mazama tephra to Middle Holocene

P2b ranges from 7633 to 5800 cal yr BP. This pollen period included samples within the upper portion of the Mazama unit and three samples above it. Only 15 taxa were identified in P2b. At the start of this zone, *Pinus* subg. *Pinus* increased abruptly from 38% to 87%, *Pinus* subg. *Strobus* remained below 1%, and *Abies* declined to 0–8%. Other taxa included Cupressaceae (1–4%), Betulaceae (1–5%), *Salix* (2–12%), *Populus* undiff. (2%), Grossulariaceae (1%), *Artemisia* (1–8%), *Ambrosia*-type (2–6%), Amaranthaceae (4–12%), Brassicaceae (2%), Solanaceae (1%), Typhaceae (0.3–1%), and Poaceae (2–6%). Only trace amounts of *Pseudotsuga* and Fabaceae were present. Pollen concentrations were low within the Mazama unit (21,000 grains/cm^3) but increased to 36,000 grains/cm^3 above the unit.

Modern pollen

The modern pollen included 14 taxa, including *Pinus* subg. *Pinus* (19%), *Pinus* subg. *Strobus* (<1%) Cupressaceae (9%), *Populus* undiff. (2%), *Quercus* (2%), *Artemisia* (31%), *Ambrosia*-type (6%), Amaranthaceae (18%), Boraginaceae (1%), Fabaceae (5%), Linaceae (2%), Plantaginaceae (1%), Typhaceae (1%), and Poaceae (3%). The modern assemblage differed from the pre-Mazama zones primarily due to the dominance of *Artemisia* sp., far lower *Pinus* subg. *Pinus*, higher Fabaceae (presumably *Medicago* [alfalfa]), and the occurrence of *Quercus*.

Coprolite pollen

The coprolite pollen assemblages were more variable and less species-rich than the sediment pollen samples (Fig. 6B). We

https://doi.org/10.1017/qua.2023.44 Published online by Cambridge University Press

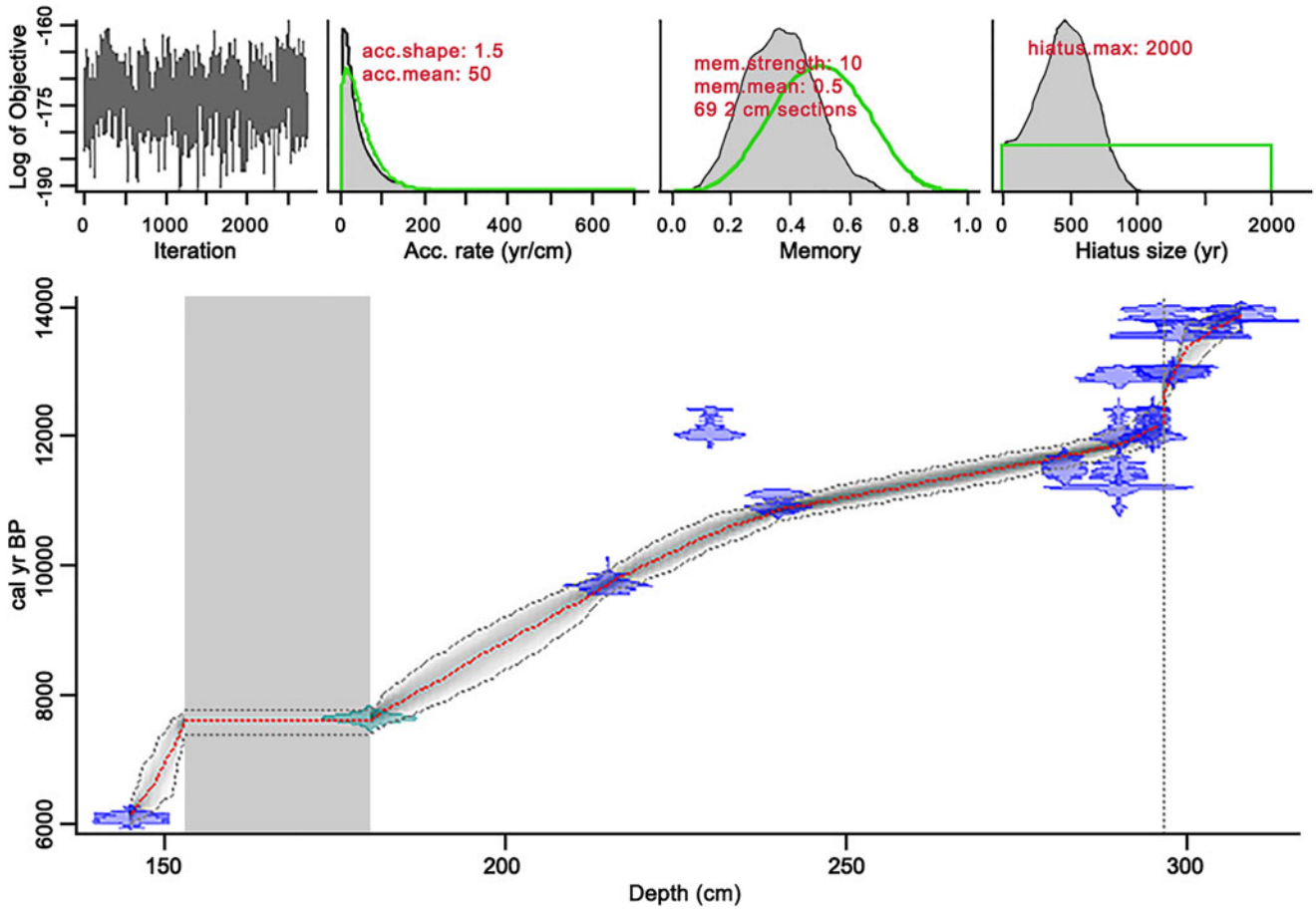

Figure 5. Bacon age–depth model for Paisley Cave 2, Unit 6 (Blaauw and Christen, 2011). The gray area on the graph represents sediments enriched with Mazama tephra. The top row of figures shows the evolution of the fit of the model, the prior and posterior distributions of the sedimentation accumulation rate, the temporal memory of the accumulation rate, and the duration of the hiatus (vertical dashed line).

describe the coprolite pollen following the same zones identified for the sediment pollen record. All coprolites analyzed postdate the hiatus in the age–depth model.

P1: Post-YD to Holocene

Seventeen pollen taxa were identified in the five analyzed coprolites from P2. These coprolites were dominated by *Pinus* subg. *Pinus* (30–70%) and *Artemisia* (14–51%) pollen. Other common pollen taxa were Poaceae (7%), Cyperaceae (5%), Amaranthaceae (4%), *Ambrosia*-type (2%), and *Alnus* (1%). Pollen concentrations ranged from 21,000 to 70,000 grains/g.

P2a: Early Holocene to Mazama tephra

Nineteen pollen taxa were identified in the 14 analyzed coprolites from P2a. These coprolites are dominated by *Pinus* subg. *Pinus* (declining from a high of 80% to 41%) and *Artemisia* (7–28%). Cupressaceae (likely representing *Juniperus*) increased from trace levels to 7%. Other common pollen taxa were Poaceae (6%), Cyperaceae (3%), Amaranthaceae (4%), *Ambrosia*-type (3%), and *Alnus* (1%). *Abies* is notably rare (<1%), and Typhaceae was overall rare but was abundant (10%) in the uppermost coprolite of this zone. Pollen concentrations were generally ca. 50,000 grains/g, but two samples (200 and 235 cm) have very high concentrations (570,000 and 110,000 grains/g, respectively).

P2b: Mazama tephra to mid-Holocene

Twenty-one pollen taxa were identified in the five analyzed coprolites from the second half of P2b. These coprolites were also dominated by *Pinus* subg. *Pinus* (21–60%) and *Artemisia* (14–26%). Other common pollen taxa were Amaranthaceae (14%), Poaceae (6%), Cupressaceae (6%), *Ambrosia*-type (4%), and Asteroideae-type (1%). Only trace amounts of *Abies*, Cyperaceae, and *Alnus* were present.

Statistical analysis

In the joint ordination of the pollen assemblages from the sediments and coprolites, the two groups do not overlap in ordination space (Fig. 7). The ordination space occupied by the sediment samples is larger than that occupied by coprolite samples, indicating greater taxonomic turnover among the sediment samples. The coprolite and sediment samples fell into distinct groups along NMDS axis 1, with coprolite samples located closer to the taxa scores for *Pinus*, Poaceae, Cupressaceae, and Cyperaceae. In contrast, the sediment samples start in the upper right and, for periods P1 and P2, decrease on NMDS axis 2 as influenced by a variety of herbaceous taxa arrayed along that axis. Sediment samples moved close to coprolite samples after the large increase in *Pinus* in the sample at 170 cm.

Examination of pollen-assemblage turnover shows the degree of change of pollen assemblages between adjacent samples for

https://doi.org/10.1017/qua.2023.44 Published online by Cambridge University Press

Table 1. Radiocarbon dates from Paisley Cave 2, unit 6.

Depth[a] (cm)	Material	Lab number	Radiocarbon age	Calibrated 2σ age range	Source
145	Amorphous coprolite plant matter	CAMS-176969	5305 ± 30	6190–5950	This study
152–180	Mazama tephra	—	—	7682–7584	Egan et al., 2015
215	*Artemisia* wood	UGAMS-14472	8740 ± 20	9890–9560	Saban, 2015
230	*Artemisia* wood	UGAMS-14473	10,310 ± 20	12,440–11,940	Saban, 2015
240	*Artemisia* wood	UGAMS-14474	9630 ± 20	11,170–10,800	Saban, 2015
282	*Artemisia* charcoal	UCIAMS-98931	10,020 ± 30	11,710–11,320	Jenkins et al., 2016
290	*Artemisia* charcoal	D-AMS 1217-410	9774 ± 46	11,260–11,110	Jenkins et al., 2016
290	*Atriplex* bark cordage	UCIAMS-85337	9995 ± 25	11,680–11,280	Jenkins et al., 2016
290	*Atriplex* bark cordage	UCIAMS-87420	10,920 ± 35	12,890–12,760	Jenkins et al., 2016
290	*Artemisia* charcoal	UCIAMS-90577	11,005 ± 30	13,060–12,830	Jenkins et al., 2016
295	Bone: Artiodactyl	UCIAMS-103089	10,290 ± 30	12,440–11,830	Jenkins et al., 2016
295	*Artemisia* wood	UCIAMS-103086	10,365 ± 30	12,470–12,000	Jenkins et al., 2016
296	Bone: *Camelops* carpal	UCIAMS-103085	11,980 ± 35	14,020–13,780	Jenkins et al., 2016
298	*Artemisia* charcoal	UCIAMS-102110	11,055 ± 35	13,090–12,850	Jenkins et al., 2016
298	*Artemisia* charcoal	D-AMS-1217-406	11,098 ± 45	13,100–12,900	Jenkins et al., 2016
299	Bone: *Equus* sp. maxilla	UCIAMS-86251	11,740 ± 25	13,740–13,500	Jenkins et al., 2016
305	Bone: unknown mammal	UCIAMS-90593	11,930 ± 25	14,010–13,610	Jenkins et al., 2016
308	Bone: Leproid humerus	D-AMS-024767	12,008 ± 35	14,020–13,800	Jenkins et al., 2016

[a]Depths are with respect to a datum at 1367.70 m elevation.

coprolites and sediments and contrasts these changes with differences between coprolites and associated sediments (Fig. 8). We found that the dissimilarity of pollen assemblages between coprolites and associated sediments (chord distance ca. 0.6) was greater than the serial dissimilarity (turnover of pollen assemblages between stratigraphically adjacent samples) within either group (chord distances ca. 0.2–0.4), supporting our first hypothesis. However, we did not find that serial dissimilarity was greater for coprolites than for sediments. Rather, the opposite pattern emerged for most of the P2 zone, thus not supporting the second hypothesis.

Pollen taxonomic richness, estimated by rarefaction to a 175-grain count, was greater in the sediment samples (mean = 11.3) than in the coprolite samples (mean = 10.2). While richness was greater in the sediment than adjacent coprolites for 20 of the 24 analyzed coprolites, a paired *t*-test showed only marginal significance ($t = -1.8$, $P = 0.08$; Fig. 9), thus not fully supporting the third hypothesis.

DISCUSSION

Pollen assemblages at Paisley Caves are influenced by the proximal sagebrush steppe, the wetlands of the Chewaucan Basin and lake edge, and the conifers of the forested uplands west of the caves. Adjacent to Paisley Caves, Summer Lake changed in size and salinity throughout the Holocene. Thus, the pollen record should also have been influenced by the changing riparian, lakeshore, and wetland vegetation through time. Surrounding these wetlands, a mix of steppe vegetation, common to the lower elevations of the NGB, graded into juniper woodlands and forest, with sharp community changes occurring within a few hundred meters of elevation, particularly in wetter areas or on north-facing aspects (Wigand and Rhode, 2002; Grayson, 2011).

The sedimentary pollen analyzed in this study represents more than 7000 yr of deposits that may reflect local climate, hydrology, and Summer Lake's transgressive and regressive shorelines. Our pollen record from cave sediments is similar to the adjacent record developed by Beck et al. (2018), with the exception of much higher *Abies* and *Salix* pollen percentages in our profile. In contrast, our mammalian coprolite pollen record differs substantially from the adjacent *Neotoma* coprolite pollen record developed by Beck et al. (2020). In the following sections, we discuss the causes of these differences and examine the environmental drivers of the changes in the sediment pollen record in the context of prior studies in the NGB.

P1: Late Pleistocene BA to Holocene

Hudson et al. (2019, 2021) characterize conditions in the Chewaucan Basin during the terminal B-A (ca. 13,000 cal yr BP) as warming with high effective moisture and a deeper lake than immediately prior, with the shoreline only 17 m below and within 100 m horizontally of the base of 5-Mile Point Butte. This time period is poorly represented in the unit 2/6 record with a modeled hiatus (Fig. 6A). As no hiatus exists in other portions of the cave, this hiatus may be due to a localized impact, such as high foot traffic. Our single pollen sample from this time contains a good representation of the riparian and lakeshore taxa of *Salix* and Typhaceae. In contrast, the high abundance of *Artemisia* and *Ambrosia*-type pollen in this zone suggests arid steppe conditions. As is the case today near riparian settings, riparian and arid steppe taxa are closely juxtaposed; our results

https://doi.org/10.1017/qua.2023.44 Published online by Cambridge University Press

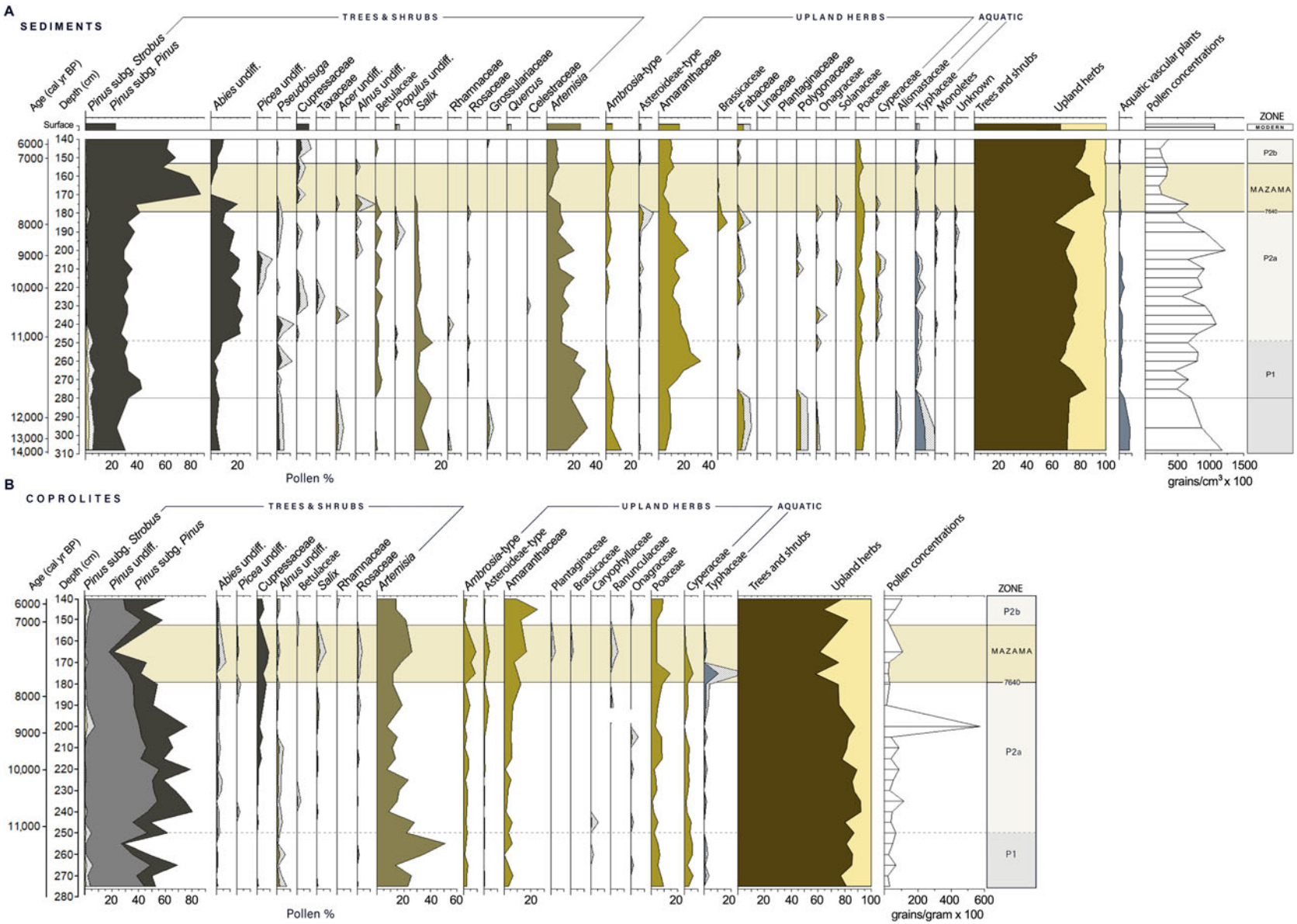

Figure 6. (**A**) Pollen diagram from cave sediments from Paisley Cave 2 Unit 6. The diagram includes a surface sample taken at 10 cm below the modern surface immediately in front of Cave 2. The depth of the modeled hiatus (296.5 cm) is shown. (**B**) Pollen diagram for pollen in coprolites located adjacent to sediment samples. Pollen concentrations are grains per gram of dry mass.

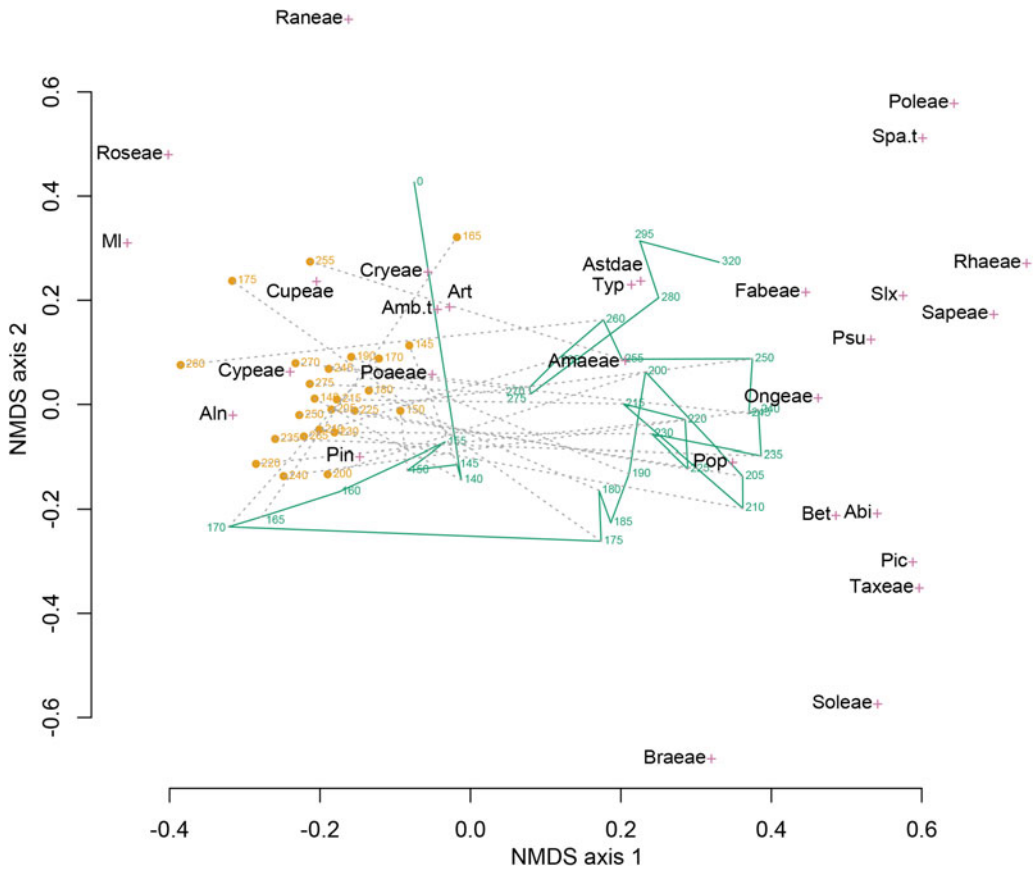

Figure 7. Nonmetric multidimensional scaling (NMDS) of the combined coprolite (orange circles) and sediment (green line) pollen assemblage data set. Sample depths (centimeters below cave floor) are shown for both coprolite and sediment samples. Green line connects sediment pollen samples in stratigraphic order. Gray dashed lines connect coprolite and adjacent sediment samples. The species scores of the 29 pollen taxa are shown by magenta crosses. Abi, *Abies*; Aln, *Alnus*; Amaeae, Amaranthaceae; Amb.t, *Ambrosia*-type; Art, *Artemisia*; Astdae, *Asteroideae*; Bet, *Betula*; Braeae, Brassicaceae; Cryeae, Caryophyllaceae; Cupeae, Cupressaceae; Cypeae, Cyperaceae; Fabeae, Fabaceae; Ml, Pteridophyta (monolete); Ongeae, Onagraceae; Pic, *Picea*; Pin, *Pinus*; Poaeae, Poaceae; Poleae, Polemoniaceae; Pop, *Populus*; Psu, *Pseudotsuga*; Raneae, Ranunculaceae; Rhaeae, Rhamnaceae; Roseae, Rosaceae; Sapeae, Sapindaceae; Slx, *Salix*; Soleae, Solanaceae; Spa.t, *Sparganium*-type; Taxeae, Taxaceae; Typ, *Typha*. Ninety percent of the variation in differences in pollen assemblages (defined by the chord distance) is explained by the two dimensions of the NMDS ordination.

are consistent with geologic evidence for freshwater being much closer to the caves than it is today. Our findings correspond well with results from other pluvial lake basins near the Chewaucan Basin, including pollen and highwater stand timings from Warner Valley to the east (Wriston and Smith, 2017) and pollen, macrobotanical analysis, and highwater stand timings from Fort Rock Basin to the north (Friedel, 1993; Egger et al., 2021; McDonough et al., 2022).

The YD is well represented archaeologically through a rich cultural assemblage (Jenkins et al., 2013, 2016), but based upon the sediment chronology, there was little sediment material from this time in our sampled Unit 6. This contrasts with Unit 4, where Beck et al. (2018) inferred a continuous record through the YD. It is possible that cave habitation and hearths eroded and consumed this layer in Unit 6. The YD is generally described as cool and dry in western North America (Mitchell, 1976; Allison, 1982; Licciardi, 2001; Vacco et al., 2005; Carlson, 2013; Jenkins et al., 2016). The YD is characterized in the Summer Lake basin as a period of cooler conditions and increased aridity, ultimately resulting in Summer Lake receding (Cohen et al., 2000; Hudson et al., 2019, 2021). After the YD, there was warming and increased effective moisture in conjunction with increasing insolation during Northern Hemisphere summers (Kutzbach et al., 1998). While the YD shorelines are poorly constrained at Summer Lake, it appears likely that Summer Lake levels rose at the start of the Holocene (Hudson et al., 2021), as has been suggested for nearby Warner Lake (Wriston and Smith, 2017).

Although truncated by a hiatus, the remainder of zone P1, from 12,100 to 11,100 cal yr BP appears consistent with the YD having been in a period of high aridity. *Artemisia* and Amaranthaceae pollen increases, and *Pinus* subg. *Pinus* decreases. Comparing the relative amounts of the two Asteraceae subgroups, *Ambrosia* spp. (ragweed) can at times be indicative of highly arid conditions (Thompson, 1996; Dennison-Budak, 2010), while the Asteroideae-types can be indicative of wetter or cooler conditions (Heusser et al., 1995; Thompson, 1996; Mudie et al., 2007). Post-YD *Ambrosia*-type asters are in high abundance until ca. 11,100 cal yr BP, indicative of continuing aridity and increasing temperatures.

Pinus subg. *Pinus* (representing *P. ponderosa* and *P. contorta*) remained fairly low (ca. 20–30%) through P1. *Pinus* species are highly prolific pollen producers, contributing significantly to the regional pollen signal (Minckley et al., 2008). While *Pinus* percentages were higher than the surface sample (Fig. 6A), they were like that of other surface pollen assemblages from Paisley Caves (Beck et al., 2018) and much lower than *Pinus* percentages

https://doi.org/10.1017/qua.2023.44 Published online by Cambridge University Press

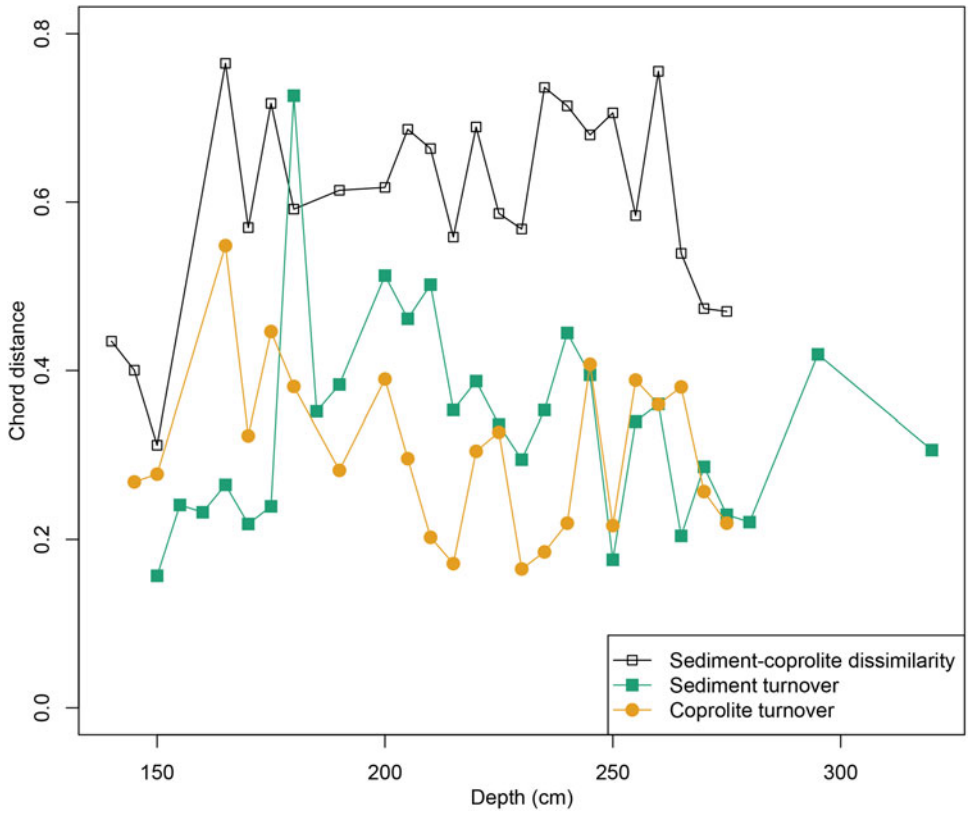

Figure 8. Dissimilarity between and within pollen assemblages of coprolites and associated sediment. Dissimilarity is measured by the chord distance. Dissimilarity between coprolites and adjacent sediment (black line) is greater than the turnover (serial dissimilarity) within coprolites or sediments.

at sites closer to current *Pinus* population (Beck et al., 2018, 2020), supporting the conclusion of Beck et al. (2020) that pines were not substantially closer than present to Paisley Caves during this period.

Highly notable is the presence of pollen from *Pinus* subg. *Strobus* (<2%) in the P1 pollen assemblage. In the NGB, this pollen type represents *Pinus albicaulis* (whitebark pine) and *Pinus monticola* (western white pine). Both species are indicative of higher moisture and lower summer temperatures than those occurring at the basin floor today, as *P. albicaulis* is found at elevations at or above 2100 m, and *P. monticola* grows between 1700 and 2000 m. The presence of *Pinus* subg. *Strobus* in P1 indicates lower aridity and cooler temperatures at lower elevations during the terminal Pleistocene relative to later periods.

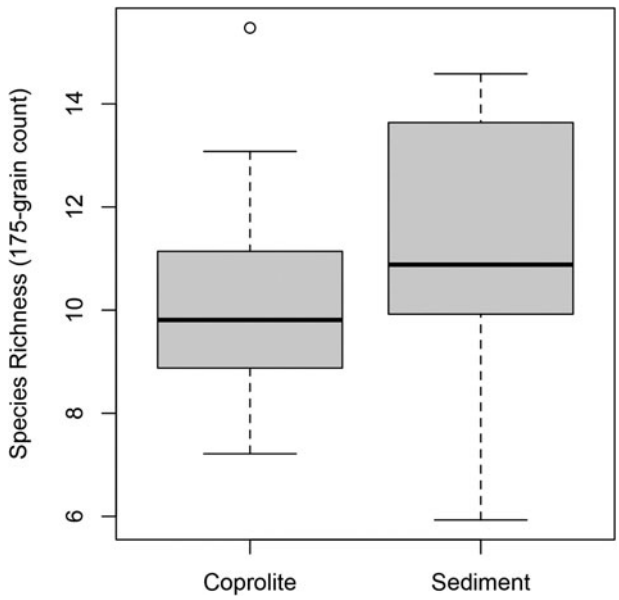

Figure 9. Pollen taxonomic richness in 24 coprolite samples and 24 adjacent sediment samples estimated by rarefaction on a 175-grain pollen count.

Also notable is the absence of Cupressaceae (*J. occidentalis*) pollen in P1 samples, indicating either low abundance of Cupressaceae in the basin during P1 or poor pollen preservation within 2/6 sediments. That Cupressaceae was present in the Summer Lake area at this time has been established, as *J. occidentalis* seeds were recovered from unit 2/6 from both pre- and post-YD deposits (Kennedy, 2018), and a trace of Cupressaceae pollen during P1 was reported by Beck et al. (2018) in a different area of Cave 2. The seeds were recovered primarily from hearth deposits and showed signs of charring (Jenkins et al., 2013; Kennedy, 2018). The presence of *Juniperus* macrobotanicals within P1 and P2 deposits was likely due to human seed transport to the caves from distances farther than those traveled by rodents and is consistent with what is known about human foraging habits at the time (Grayson, 1993; Longland and Ostoja, 2013; Kennedy, 2018).

P2a: Early Holocene to the eruption of Mount Mazama

P2a covers the period from 11,100 to 7633 cal yr BP. Summer Lake levels were moderately high during the Early Holocene (Hudson et al., 2019, 2021), but after 9000 cal yr BP, lake levels receded rapidly. Pollen-based climate reconstruction from other

https://doi.org/10.1017/qua.2023.44 Published online by Cambridge University Press

regional sites show that temperature and aridity peaked at ca. 9000 cal yr BP (Mehringer, 1987; Minckley et al., 2007). However, the Paisley pollen record for P2a shows increased and sustained high *Abies* pollen (ca. 20%, from 11,000 to 8000 cal yr BP) and periods of elevated *Picea* and Cyperaceae pollen (>3%), while more arid-adapted taxa (Amaranthaceae and *Artemisia*) remain steady at ca. 20%.

Abies grandis × *concolor* (white fir) is currently present on Winter Rim between 1700 and 2000 m. A decrease in temperature and fire episodes would facilitate the expansion of *Abies* below 1700 m. *Abies grandis* × *concolor* is a shade-tolerant species when young and can remain in the understory for many years until a disturbance opens the tree canopy, after which rapid growth can ensue (Lanner, 1984; Howard and Aleksoff, 2000; Arno, 2007). Reduced fire frequency would also favor *Abies* relative to *Pinus*.

An alternative explanation for the increase in *Abies*, a pollen grain that is poorly dispersed due to its thick exine (Bagnall, 1975), is increased westerly flow during the pollen-producing season. Increased westerly flow, due to a deepening low pressure over the NGB, may have more effectively transported *Abies* pollen the >20 km from its nearest populations located at higher elevations. Changing strength in westerlies has been invoked to explain an increasing occurrence of *Tsuga heterophylla* (coastal western hemlock) pollen in interior British Columbia between 9000 and 8200 cal yr BP (Spooner et al., 2003).

Picea peaks at 9000 cal yr BP during the P2a period. Beck et al. (2018) reported very low *Abies* and *Picea* pollen percentages from the unit 2/4, and *Picea* was also reported from higher-elevation sites such as Deadhorse Lake (2200 m elevation) on Gearhart Mountain (2440 m elevation) 30 km south of Paisley (Minckley et al., 2007). It is probable that the *Picea* pollen at Paisley Caves originated from Gearhart Mountain.

Typhaceae species are associated with marshy, perennially wet areas. Typhaceae counts decreased throughout P2 and remained low after the Mazama eruption. Waning Typhaceae concentrations in the sediments is a clear indicator of Summer Lake recession moving marshy areas further away from the caves. *Typha latifolia* and *Typha angustifolia* are both currently present in the Summer Lake basin, but *T. latifolia* occurs at a far higher abundance. The genus *Sparganium* has recently been added to the Typhaceae family, with *Sparganium euricarpum* present in Summer Lake Marsh. While *Sparganium* pollen is distinct from *Typha*, we merged it into Typhaceae, as it was only present in the lowermost two samples. Both genera occupy similar wetland habitats, although *Sparganium* requires deeper water than *Typha* sp. (Dennis and Halse, 2008).

P2b: Mazama tephra to mid-Holocene

P2b (7633–5800 cal yr BP) includes sediments from the Mazama tephra unit. The presence of sedimentary pollen and the occurrence of coprolites within the Mazama tephra unit suggest downward percolation of pollen and/or multiple tephra deposition events. In all sediments other than the Mazama unit, the cave sediment is dense and cemented by *Neotoma* fecal pellets. However, the Mazama tephra is coarse (>1 mm grain size) and loosely consolidated, with no cementation. This would suggest the pollen stratigraphy within the ca. 26-cm-deep tephra units is mixed. However, we also found an abrupt increase of *Pinus* within the tephra layer, perhaps attributable to Mazama deposition occurring in at least two phases (Buckland et al., 2020). In a study of pollen concentration of the Mazama tephra, Mehringer et al. (1977) interpreted an increase in *Pinus* pollen from 10 to 60% as an initial, rapidly deposited tephra layer followed by a second event during the *Pinus* pollen season. The pattern of pollen in the Paisley Cave Mazama unit is consistent with multiple ash depositions in different seasons (Mehringer, 1987; Egan et al., 2015). However, the coprolite assemblages do not show a similar increase in *Pinus* as would be expected if the tephra affected the regional vegetation.

The remainder of P2b shows an increase in Cupressaceae, likely indicating an increase in juniper woodland in the middle Holocene, as well as an increase in *Abies*. Some herbaceous plant types, such as Brassicaceae and Fabaceae, thrived in response to the tephra deposition. Such plants have adaptations to disturbance, including, in the case of Fabaceae, the ability to fix nitrogen from the atmosphere.

Coprolite pollen assemblages

The amount of pollen present within a coprolite reflects seasonality and the natural pollen rain; various dispersal forms, including anemophily (wind dispersed), entomophily (insect dispersed), and zoophily (animal dispersed); the types of plants contributing to ambient pollen; and the amount of pollen output by different plant species (Shillito et al., 2020). Intake into an organism's mucus system occurs either through passive or intentional ingestion. Passive ingestion occurs through respiration, drinking water with pollen present, eating plant materials with pollen present on the plant surfaces (Wood et al., 2012; Shillito et al., 2020), or through the predation and consumption of the digestive organs of plant-consuming prey (Carrión et al., 2001). Pollen has also been intentionally ingested as a food source by Native American people throughout North America, with examples including *Typha* and *Populus* pollen used as food seasoning and thickeners, as well as used in cultural customs and rites (Williams-Dean and Bryant, 1975; Euler, 1986).

Our hypotheses regarding the pollen assemblages of coprolite versus sediment samples were largely supported. First, the dissimilarity between sediment and coprolite pollen assemblages (chord distance between coprolite and associated sediments) was much greater than the serial dissimilarity (chord distance between stratigraphically adjacent samples) within sediments or coprolites (Figs. 7 and 8). This pattern is expected because the sediment pollen assemblage represents a larger area over a longer time, thus capturing regional pollen more consistently. The coprolite assemblage represents a brief temporal window, while the sediment assemblage integrates a decade or more of pollen deposition. Second, the serial turnover among coprolites was not greater than that among sediments. We hypothesized that the sampling of pollen by a foraging human or another large mammal would result in a stochastic pattern from feces "spiked" with variable amounts of pollen in the gut that were inhaled and ingested, while cave sediment pollen represents a much greater spatial and temporal smoothing. However, the turnover in coprolite assemblages was often less than that in sediment samples. Such a pattern might result from a selection of certain pollen types from the environment based on foraging or hunting behaviors. Third, pollen taxonomic diversity was slightly lower in the coprolites than in the sediment samples. This is consistent with sediment samples representing many years of pollen accumulation from a broad regional source, while the coprolite pollen samples only a portion of the landscape and over a brief period of time.

Compared with sediment pollen assemblages, the coprolite pollen has higher abundances of lighter pollen types (*Pinus*,

https://doi.org/10.1017/qua.2023.44 Published online by Cambridge University Press

Cupressaceae, and in P1 and P2b, *Artemisia*) and wetland pollen types (Cyperaceae, and in P2b, Typhaceae) and lower abundances of heavy pollen types, including *Abies*, *Pseudotsuga*, and Amaranthaceae. The higher occurrence of lighter pollen types (e.g., *Pinus* relative to *Abies*) in the coprolites than in the sediments is consistent with pollen being inhaled, then moved into the gut by mucus transport. Pollen that remains airborne for longer periods would be more likely to be inhaled. Seasonality may also play a role in the coprolite pollen assemblages. For example, the high abundance of *Artemisia* in some coprolites may be due to seasonal use of the caves timed with the late-summer flowering of *Artemisia*. As the production of *Pinus* and the other regional conifers all occur in the late spring months (Burns and Honkala, 1990; Osmond et al., 1990), we can surmise that there were two seasonal occupational periods of the caves. Further, all of the coprolites examined for this study contained pollen, suggesting no winter occupation of Cave 2.

The higher abundances of wetland taxa, such as Cyperaceae, in coprolites than in sediments is best explained by people and other animals traveling to marsh areas and ingesting pollen in water. The fact that this difference between coprolites and sediments was observed for all time periods suggests that the phenomenon occurred regardless of the distance of the wetlands from the caves. *Typha* pollen has similar abundance (~0.5–2%) in sediment and coprolites, with the exception of one coprolite with 10% *Typha* pollen. This particularly high abundance of *Typha* may be attributable to intentional consumption of *Typha* pollen, as was practiced by the Native people of the region (Euler, 1986).

Cupressaceae (*Juniperus*) pollen percentages are higher in coprolites than in sediments throughout zones P2a and P2b. This could indicate intentional human or other large mammal interaction with *Juniperus* woodlands some distance from the caves. This is consistent with human activity at the time, as *Juniperus* was an important dietary and medicinal resource (Euler, 1986; Kennedy, 2018). This is also consistent with the seasonal timing of *Pinus* pollination in late spring, as *J. occidentalis* also begin producing cones in late spring (Miller and Rose, 1995; Adams, 2019). An increase in Cupressaceae through the Early Holocene has not been described before in the NGB (Miller and Wigand, 1994). The increase may represent either an expansion of *Juniperus* woodlands, the increased use of juniper woodlands by humans or other large mammals, or both.

The Amaranthaceae pollen present in Cave 2 coprolites is likely derived from an alkaline-tolerant *Chenopodium*. During P1 and P2a, this taxon has low abundance in the coprolites, while in P2b, there is an increased amount relative to the sediments. This change may indicate a change from avoidance of saltbush-dominated playa areas to increased travel through such areas as playas increased in extent through the Early Holocene. The organism that ingested the pollen would have done so in early to midsummer when *Atriplex* pollen is produced (Hitchcock and Cronquist, 2018).

The concentration of pollen in the coprolites varied, with the majority being relatively low pollen concentration, indicative of passive pollen ingestion. There is a major spike in pollen in a coprolite at 200 cm (8800 cal yr BP), matching a spike in sediment pollen concentration at the same depth. The coprolite spike was driven by a high *Pinus* influx, while the sedimentary spike was the result of high *Artemisia* and Amaranthaceae pollen, perhaps reflecting a brief cold period. Perhaps the coprolite producer was near *Pinus* stands, as such places may have provided mesic conditions at a time when Summer Lake was all but desiccated (Cohen et al., 2000; Friedel, 1993; Licciardi, 2001; Hudson et al., 2021).

CONCLUSIONS

The pollen record from Paisley Cave 2 in south-central Oregon is consistent with prior studies showing steppe conditions persisting throughout much of the Northern Great Basin during the Pleistocene and into the Holocene (Mehringer, 1986). However, differences in climate, the presence of large freshwater lakes, and changes in insolation timing and intensity mean that there are no analogous ecological conditions today for the region.

By contrasting the degree of changes between adjacent pollen sample types, this study found that the dissimilarity of pollen assemblages between coprolites and associated sediments was greater than the serial dissimilarity between stratigraphically adjacent samples within either group. However, serial dissimilarity within types was not greater for coprolites than sediments. The coprolites showed localized pollen assemblages related to mammalian survival strategies within a 1–2 day period, resulting in less taxonomic variability over time than sedimentary pollen.

Survival decision making by the coprolite producers is suggested by the high percentage of aquatic/wetland pollen in the coprolites. As large mammals need to drink water frequently, as do potential prey animals, it is reasonable to assume the water sources would be in relatively closer proximity to the caves. Overall, the coprolite pollen shows a strong seasonal signal, with late spring and late summer equally strong, but there are components of early spring and midsummer as well. If the coprolite producers were present at Paisley Cave in late fall or winter, we would expect very low pollen concentration in the coprolites, which was not the case for any of the coprolite samples.

Taphonomy and careful excavations at Paisley Caves have provided the rare opportunity to analyze two pollen taphonomies from the same location. Rarer still was to have both preserved in a long chronological sequence. Pollen from cave sediments can provide a regional environmental reconstruction over time (White, 2007), but it is by contrasting sediment pollen with chronologically related coprolite pollen that additional angles of ecological interactions related to changing climates and ecosystems can be determined. The results of these types of studies can then be applied to questions regarding diet, health, mobility, and other topics relating to past human or other mammalian behaviors.

Acknowledgments. The completion of this article was made possible through the Rippey Graduate Writing Grant received through the Department of Geography at the University of Oregon. We thank Brianna Rollo, R. P. Cromwell, Pat Luther, Matthew Kale, and Olga Saban-Kaup for their contribution to this research. We thank W.W. Oswald and three anonymous reviewers for their comments on the article.

Conflict of Interest Statement. The authors declare no conflict of interest.

REFERENCES

Adams, R.P., 2019. *Juniperus* of Canada and the United States: taxonomy, key and distribution. *Lundellia* **21**, 1–34.

Allison, I.S., 1982. *Geology of Pluvial Lake Chewaucan, Lake County, Oregon*. Oregon State University Press, Corvallis. ir.library.oregonstate.edu/xmlui/handle/1957/21983, accessed February 11, 2013.

Anderson, E.W., Borman, M.M., Krueger, W.C., 1998. *The Ecological Provinces of Oregon: A Treatise on the Basic Ecological Geography of the State*. Technical Report. Oregon Agricultural Experiment Station, Corvallis.

https://doi.org/10.1017/qua.2023.44 Published online by Cambridge University Press

Anderson, R.Y., 1955. Pollen analysis, a research tool for the study of cave deposits. *American Antiquity* **21**, 84–85.

Arno, S.F., 2007. *Northwest Trees*. 2nd ed. Mountaineers Books, Seattle.

Badger, T.C., Watters, R.J., 2004. Gigantic seismogenic landslides of Summer Lake basin, south-central Oregon. *Geological Society of America Bulletin* **116**, 687–697.

Bagnell, C.R., Jr., 1975. Species distinction among pollen grains of *Abies*, *Picea*, and *Pinus* in the Rocky Mountain area (a scanning electron microscope study). *Review of Palaeobotany and Palynology* **19**, 203–220.

Bartlein, P.J., Anderson, K.H., Anderson, P.M., Edwards, M.E., Mock, C.J., Thompson, R.S., Webb, R.S., Whitlock, C., 1998. Paleoclimate simulations for North America over the past 21,000 years: features of the simulated climate and comparisons with paleoenvironmental data. *Quaternary Science Reviews* **17**, 549–585.

Bartlein, P.J., Harrison, S.P., Brewer, S., Connor, S., Davis, B.A.S., Gajewski, K., Guiot, J., *et al.*, 2011. Pollen-based continental climate reconstructions at 6 and 21 ka: a global synthesis. *Climate Dynamics* **37**, 775–802.

Beck, C.W., Bryant, V.M., Jenkins, D.L., 2018. Analysis of Younger Dryas—Early Holocene pollen in sediments of Paisley Cave 2, south-central Oregon. *Palynology* **42**, 168–179.

Beck, C.W., Bryant, V.M., Jenkins, D.L., 2020. Comparison of *Neotoma* (packrat) feces to associated sediments from Paisley Caves, Oregon, U.S.A. *Palynology* **44**, 723–741.

Bennett, K.D., 1996. Determination of the number of zones in a biostratigraphic sequence. *New Phytologist* **132**, 155–170.

Benson, L., Kashgarian, M., Rye, R., Lund, S., Paillet, F., Smoot, J., Kester, C., Mensing, S., Meko, D., Lindström, S., 2002. Holocene multidecadal and multicentennial droughts affecting Northern California and Nevada. *Quaternary Science Reviews* **21**, 659–682.

Blaauw, M., Christen, J.A., 2011. Flexible paleoclimate age-depth models using an autoregressive gamma process. *Bayesian Analysis* **6**, 457–474.

Blong, J.C., Adams, M.E., Sanchez, G., Jenkins, D.L., Bull, I.D., Shillito, L.-M., 2020. Younger Dryas and early Holocene subsistence in the northern Great Basin: multiproxy analysis of coprolites from the Paisley Caves, Oregon, USA. *Archaeological and Anthropological Sciences* **12**, 224.

Bryant, V.M., 1974. Prehistoric diet in southwest Texas: the coprolite evidence. *American Antiquity* **39**, 407–420.

Bryant, V.M., Reinhard, K.J., 2012. Coprolites and archaeology: the missing links in understanding human health. In: Hunt, A.P., Milan, J., Lucas, S.G., Spielmann, J.A. (Eds.), *Vertebrate Coprolites, Bulletin 57*. New Mexico Museum of Natural History and Science, Albuquerque, pp. 379–387.

Bryant, V.M., Jr., Holloway, R.G., 1983. The role of palynology in archaeology. *Advances in Archaeological Method and Theory* **6**, 191–224.

Buckland, H.M., Cashman, K.V., Engwell, S.L., Rust, A.C., 2020. Sources of uncertainty in the Mazama isopachs and the implications for interpreting distal tephra deposits from large magnitude eruptions. *Bulletin of Volcanology* **82**, 23.

Burns, R.M., Honkala, B.H., 1990. *Silvics Manual*. Vol. 1, *Conifers*. Agriculture Handbook 654. Forest Service, U.S. Department of Agriculture, Washington, DC. srs.fs.usda.gov/pubs/misc/ag_654/table_of_contents.htm, accessed August 7, 2022.

Carlson, A.E., 2013. Paleoclimate: the Younger Dryas climate event. In: Elias, S.A. (Ed.), *Encyclopedia of Quaternary Science*. Vol. 3. Elsevier, Amsterdam, pp. 126–134.

Carrión, J.S., Riquelme, J.A., Navarro, C., Munuera, M., 2001. Pollen in hyaena coprolites reflects late glacial landscape in southern Spain. *Palaeogeography, Palaeoclimatology, Palaeoecology* **176**, 193–205.

Carter, V.A., Brunelle, A., Minckley, T.A., Shaw, J.D., DeRose, R.J., Brewer, S., 2017. Climate variability and fire effects on quaking aspen in the central Rocky Mountains, USA. *Journal of Biogeography* **44**, 1280–1293.

Chame, M., 2003. Terrestrial mammal feces: a morphometric summary and description. *Memórias do Instituto Oswaldo Cruz* **98**(Suppl. 1), 71–94.

Cohen, A., Palacios-Fest, M., Negrini, R., Wigand, P., Erbes, D., 2000. A paleoclimate record for the past 250,000 years from Summer Lake, Oregon, USA: II. Sedimentology, paleontology and geochemistry. *Journal of Paleolimnology* **24**, 151–182.

Cressman, L.S., 1940. Studies on early man in south central Oregon. In: *Carnegie Institution of Washington Year Book No. 39*. Carnegie Institution, Washington, DC, pp. 300–306.

Cronquist, A., Holmgren, A.H., Holmgren, N.H., Reveal, J.L., 1972. *Intermountain Flora; Vascular Plants of the Intermountain West, U.S.A.* Hafner Publishing, New York Botanical Garden, New York.

Dennis, L.R.J., Halse, R.R., 2008. *Aquatic and Wetland Plants of Oregon with Vegetative Key*. 1st ed. Uncial Press, Beaverton, OR.

Dennison-Budak, C.W., 2010. Ostracodes as Indicators of the Paleoenvironment in the Pliocene Glenns Ferry Formation, Glenns Ferry Lake, Idaho. Master's thesis, Kent State University, Kent, OH. https://etd.ohiolink.edu/acprod/odb_etd/ws/send_file/send?accession=kent1271442702&disposition=inline, accessed April 18, 2014.

Dexter, J., Saban, C.V., 2014. Assessing Late Pleistocene to Early Holocene diet breadth in the northern Great Basin through paleoethnobotanical analysis. Presented at the 79th Annual Meeting of the Society for American Archaeology, April 23–27, 2014, Austin, TX.

Egan, J., Staff, R., Blackford, J., 2015. A high-precision age estimate of the Holocene Plinian eruption of Mount Mazama, Oregon, USA. *The Holocene* **25**, 1054–1067.

Egger, A.E., Ibarra, D.E., Weldon, R., Langridge, R.M., Marion, B., Hall, J., 2021. Influence of pluvial lake cycles on earthquake recurrence in the northwestern Basin and Range, USA. In: Starratt, S.W., Rosen, M.R. (Eds.), *From Saline to Freshwater: The Diversity of Western Lakes in Space and Time*. Geological Society of America, McLean, VA, pp. 1–28.

Euler, R.C., 1986. The Great Basin. In: D'Azevedo, W.L., Sturtevant, W.C. (Eds.), *Handbook of North American Indians*. Vol. 11. Smithsonian Institution Press, Washington, DC. pp. 79, 474.

Faegri, K., Kaland, P.E., Krzywinski, K., 1989. *Textbook of Pollen Analysis*. 4th ed. Blackburn Press, Caldwell, NJ.

Franklin, J. F., Dyrness, C.T., 1988. *Natural Vegetation of Oregon and Washington*. Oregon State University Press, Corvallis.

Friedel, D.E., 1993. *Chronology and Climatic Controls of Late Quaternary Lake-level Fluctuations in Chewaucan, Fort Rock, and Alkali Basins, South-Central Oregon*. Doctoral dissertation, University of Oregon, Eugene.

Gasche, H., Tunca, Ö., 1983. Guide to archaeostratigraphic classification and terminology: definitions and principles. *Journal of Field Archaeology* **10**, 325–335.

Gilbert, M.T.P., Jenkins, D.L., Gotherstrom, A., Naveran, N., Sanchez, J.J., Hofreiter, M., Thomsen, P.F., *et al.*, 2008. DNA from Pre-Clovis human coprolites in Oregon, North America. *Science* **320**, 786–789.

Grayson, D.K., 1993. *The Desert's Past: A Natural Prehistory of the Great Basin*. 1st ed. Smithsonian Institution Press, Washington, DC.

Grayson, D.K., 2011. *The Great Basin: A Natural Prehistory*. University of California Press. Berkeley.

Heizer, R.F., 1969. Analysis of human coprolites from a dry Nevada Cave. *Papers in Great Basin Archaeology, California Archaeological Survey Report* **70**, 1–20.

Heizer, R.F., Napton, L.K., Dunn, F.L., Follett, W.I., Morbeck, M.E., Radovsky, F.J., Watkins, R., 1970. *Archaeology and the Prehistoric Great Basin Lacustrine Subsistence Regime as Seen from Lovelock Cave, Nevada*. Contributions of the University of California Archaeological Research Facility, 10. University of California, Berkeley. escholarship.org/uc/item/0p60j7gf, accessed May 13, 2020.

Heusser, C.J., Denton, G.H., Hauser, A., Andersen, B.G., Lowell, T.V., 1995. Quaternary pollen record from the Archipiélago de Chiloé in the context of glaciation and climate. *Revista Geolocica de Chile* **22**, 25–46.

Hitchcock, C.L., Cronquist, A., 2018. *Flora of the Pacific Northwest: An Illustrated Manual*. 2nd ed. University of Washington Press, Seattle.

Hofreiter, M., Poinar, H.N., Spaulding, W.G., Bauer, K., Martin, P.S., Possnert, G., Pääbo, S., 2000. A molecular analysis of ground sloth diet through the last glaciation. *Molecular Ecology* **9**, 1975–1984.

Howard, J.L., Aleksoff, K.C., 2000. Abies grandis. In: *Fire Effects Information System*. U.S. Department of Agriculture, Forest Service, Rocky Mountain Research Station, Fire Sciences Laboratory, Missoula, MT. https://www.fs.usda.gov/database/feis/plants/tree/abigra/all, accessed June 28, 2022.

Hudson, A.M., Emery-Wetherell, M.M., Lubinski, P.M., Butler, V.L., Grimstead, D.N., Jenkins, D.L., 2021. Reconstructing paleohydrology

https://doi.org/10.1017/qua.2023.44 Published online by Cambridge University Press

in the northwest Great Basin since the last deglaciation using Paisley Caves fish remains, Oregon, U.S.A. *Quaternary Science Reviews* **262**, 106936.

Hudson, A.M., Hatchett, B.J., Quade, J., Boyle, D.P., Bassett, S.D., Ali, G., De los Santos, M.G., 2019. North-south dipole in winter hydroclimate in the western United States during the last deglaciation. *Scientific Reports* **9**, 4826.

Jenkins, D.L., Connolly, T.J., Aikens, C.M., 2004. Early and Middle Holocene archaeology in the northern Great Basin: dynamic natural and cultural ecologies. In: Jenkins, D.L., Connolly, T.J., Aikens, C.M. (Eds.), *Early and Middle Holocene Archaeology of the Northern Great Basin*. University of Oregon Anthropological Papers 62. Museum of Natural History and Department of Anthropology, University of Oregon, Eugene, pp. 1–20.

Jenkins, D.L., Davis, L.G., Stafford T., Jr., Campos, P.F., Connolly, T.J., Cummings, L.S., Hofreiter, M., *et al.*, 2013. Geochronology, archaeological context, and DNA at the Paisley Caves. In: Graf, K.E., Ketron, C.V., Waters, M.R. (Eds.), *Paleoamerican Odyssey*. Texas A&M Publishing, College Station, pp. 173–197.

Jenkins, D.L., Davis, L.G., Stafford, T.W., Campos, P.F., Hockett, B., Jones, G.T., Cummings, L.S., *et al.*, 2012. Clovis age western stemmed projectile points and human coprolites at the Paisley Caves. *Science* **337**, 485–510.

Jenkins, D.L., Davis, L.G., Jr., Stafford, T.W., Jr., Connolly, T.J., Jones, G.T., Rondeau, M., Cummings, L.S., *et al.*, 2016. Younger Dryas archaeology and human experience at the Paisley Caves in the northern Great Basin. In: Kornfeld, M., Huckell, B.B. (Eds.), *Stones, Bones, and Profiles: Exploring Archaeological Context, Early American Hunter-Gatherers, and Bison*. University Press of Colorado, Denver. pp. 127–205.

Kelso, G., Solomon, A., 2006. Applying modern analogs to understand the pollen content of coprolites. *Palaeogeography, Palaeoclimatology, Palaeoecology* **237**, 80–91.

Kelso, G.K., 1971. Hogup Cave, Utah: Comparative Pollen Analysis of Human Coprolites and Cave Fill. MA thesis, University of Arizona, Tucson.

Kennedy, J., 2018. A Paleoethnobotanical Approach to 14,000 Years of Great Basin Prehistory: Assessing Human-Environmental Interactions Through the Analysis of Archaeological Plant Data at Two Oregon Rockshelters. PhD dissertation, University of Oregon, Eugene. scholarsbank.uoregon.edu/xmlui/handle/1794/23918, accessed February 19, 2022.

Kovalchik, B.L., Chitwood, L.A., 1990. Use of geomorphology in the classification of riparian plant associations in mountainous landscapes of central Oregon. *Forest Ecology and Management* **33–34**, 405–418.

Kutzbach, J., Gallimore, R., Harrison, S., Behling, P., Selin, R., Laarif, F., 1998. Climate and biome simulations for the past 21,000 years. *Quaternary Science Reviews* **17**, 473–506.

Lanner, R.M., 1984. *Trees of the Great Basin: A Natural History*. University of Nevada Press. Reno.

Licciardi, J.M., 2001. Chronology of latest Pleistocene lake-level fluctuations in the pluvial Lake Chewaucan basin, Oregon, USA. *Journal of Quaternary Science* **16**, 545–553.

Long, C.J., Shinker, J.J., Minckley, T.A., Power, M.J., Bartlein, P.J., 2019. A 7600 yr vegetation and fire history from Anthony Lake, northeastern Oregon, USA, with linkages to modern synoptic climate patterns. *Quaternary Research* **91**, 705–713.

Longland, W.S., Ostoja, S.M., 2013. Ecosystem services from keystone species: diversionary seeding and seed-caching desert rodents can enhance Indian ricegrass seedling establishment. *Restoration Ecology* **2**, 285–291.

Loud, L.L., Harrington, M.R., 1929. *Lovelock Cave*. University of California Press, Berkeley. archive.org/details/LovelockCaveLoudAndHarrington1929, accessed May 13, 2020.

Mayewski, P.A., Meeker, L.D., Whitlow, S., Twickler, M.S., Morrison, M.C., Alley, R.B., Bloomfield, P., Taylor, K., 1993. The atmosphere during the Younger Dryas. *Science* **261**, 195–197.

McDonough, K., Kennedy, J., Rosencrance, R., Holcomb, J., Jenkins, D.L., Puseman, K., 2022. Expanding Paleoindian diet breadth: paleoethnobotany of Connley Cave 5, Oregon, USA. *American Antiquity* **87**, 303–332.

McDonough, K., Luthe, I., Swisher, M.E., Jenkins, D.L., O'Grady, P., White, F., 2012. ABCs at the Paisley Caves: artifact, bone, and coprolite distributions in pre-Mazama deposits. *Current Archaeological Happenings in Oregon* **37**, 7–12.

McDonough, K.N., 2019. Middle Holocene menus: dietary reconstruction from coprolites at the Connley Caves, Oregon, USA. *Archaeological and Anthropological Sciences* **11**, 5963–5982.

Mehringer, P., 1986. Prehistoric environments. In: D'Azevedo, W.L., Sturtevant, W.C. (Eds.), *Handbook of North American Indians*. Vol. 11. Smithsonian Institution Press, Washington, DC, pp. 31–50.

Mehringer, P.J., 1987. *Late Holocene Environments on the Northern Periphery of the Great Basin*. Final Report to the Bureau of Land Management, Oregon State Office. Departments of Anthropology and Geology, Washington State University, Seattle. archive.org/details/lateholoceneenvi9157mehr, accessed August 17, 2017.

Mehringer, P.J., Arno, S.F., Petersen, K.L., 1977. Postglacial history of Lost Trail Pass Bog, Bitterroot Mountains, Montana. *Arctic and Alpine Research* **9**, 345–368.

Mensing, S.A., Benson, L.V., Kashgarian, M., Lund, S., 2004. A Holocene pollen record of persistent droughts from Pyramid Lake, Nevada, USA. *Quaternary Research* **62**, 29–38.

Mensing, S.A., Sharpe, S.E., Tunno, I., Sada, D.W., Thomas, J.M., Starratt, S., Smith, J., 2013. The Late Holocene Dry Period: multiproxy evidence for an extended drought between 2800 and 1850 cal yr BP across the central Great Basin, USA. *Quaternary Science Reviews* **78**, 266–282.

Miller, R.F., Rose, J.A., 1995. Historic expansion of *Juniperus occidentalis* (western juniper) in southeastern Oregon. *The Great Basin Naturalist* **55**, 37–45. jstor.org/stable/41712862.

Miller, R.F., Wigand, P.E., 1994. Holocene changes in semiarid pinyon-juniper woodlands. *BioScience* **44**, 465–474.

Minckley, T.A., Bartlein, P.J., Whitlock, C., Shuman, B.N., Williams, J.W., Davis, O.K., 2008. Associations among modern pollen, vegetation, and climate in western North America. *Quaternary Science Reviews* **27**, 1962–1991.

Minckley, T.A., Whitlock, C., Bartlein, P.J., 2007. Vegetation, fire, and climate history of the northwestern Great Basin during the last 14,000 years. *Quaternary Science Reviews* **26**, 2167–2184.

Mitchell, V.L., 1976. The regionalization of climate in the western United States. *Journal of Applied Meteorology* **15**, 920–927.

Mudie, P.J., Marret, F., Aksu, A.E., Hiscott, R.N., Gillespie, H., 2007. Palynological evidence for climatic change, anthropogenic activity and outflow of Black Sea water during the late Pleistocene and Holocene: centennial-to decadal-scale records from the Black and Marmara Seas. *Quaternary International* **167–168**, 73–90.

Nowak, C.L., Nowak, R.S., Tausch, R.J., Wigand, P.E., 1994. Tree and shrub dynamics in northwestern Great Basin woodland and shrub steppe during the late-Pleistocene and Holocene. *American Journal of Botany* **81**, 265–277.

Oksanen, J., Blanchet, F.G., Kindt, P., McGlinn, D., Minchin, P.R., O'Hara, R.B., Simpson, G. L., Solymos, P.M., Stevens, H.H., Szoecs, E., Wagner, H., 2020. vegan: community ecology package, R package version 2.5-7. *CRAN.R-project.org/package=vegan, accessed August* **6**, 2022.

Orr, E.L., Orr, W.N., 2012. *Oregon Geology*. 6th ed. Oregon State University Press, Corvallis.

Osmond, C.B., Hidy, G.M., Pitelka, L.F., 1990. *Plant Biology of the Basin and Range*. Ecological Studies, Vol. 80. Springer, Berlin. link.springer.com/book/10.1007/978-3-642-74799-1.

Pearsall, D.M., 2016. *Paleoethnobotany: A Handbook of Procedures*. 3rd ed. Routledge, New York.

Rasmussen, S.O., Bigler, M., Blockley, S.P., Blunier, T., Buchardt, S.L., Clausen, H.B., Cvijanovic, I., *et al.*, 2014. A stratigraphic framework for abrupt climatic changes during the Last Glacial period based on three synchronized Greenland ice-core records: refining and extending the INTIMATE event stratigraphy. *Quaternary Science Reviews* **106**, 14–28.

Reimer, P.J., Austin, W.E.N., Bard, E., Bayliss, A., Blackwell, P.G., Ramsey, C.B., Butzin, M., *et al.*, 2020. The IntCal20 Northern Hemisphere Radiocarbon Age Calibration Curve (0–55 cal kBP). *Radiocarbon* **62**, 725–757.

Reinemann, S.A., Porinchu, D.F., Bloom, A.M., Mark, B.G., Box, J.E., 2009. A multi-proxy paleolimnological reconstruction of Holocene climate conditions in the Great Basin, United States. *Quaternary Research* **72**, 347–358.

https://doi.org/10.1017/qua.2023.44 Published online by Cambridge University Press

Riley, T., 2008. Diet and seasonality in the Lower Pecos: evaluating coprolite data sets with cluster analysis. *Journal of Archaeological Science* **35**, 2726–2741.

Saban, C.V., 2015. *Palynological Perspectives on Younger Dryas to Early Holocene Human Ecology at Paisley Caves, Oregon*. Master's thesis, Oregon State University, Corvallis. https://ir.library.oregonstate.edu/concern/graduate_thesis_or_dissertations/2801pk70d, accessed February 10, 2023.

Shillito, L-M., Blong, J.C., Green, E.J., and van Asperen, E.N., 2020. The what, how and why of archaeological coprolite analysis. *Earth-Science Reviews* **207**, 103196.

Shillito, L.-M., Bull, I.D., Matthews, W., Almond, M.J., Williams, J.M., Evershed, R.P., 2011. Biomolecular and micromorphological analysis of suspected faecal deposits at Neolithic Çatalhöyük, Turkey. *Journal of Archaeological Science* **38**, 1869–1877.

Smith, S.J., 1998. Processing pollen samples from archaeological sites in the southwestern United States: an example of differential recovery from two heavy liquid gravity separation procedures. In: Wrenn, J.H., Bryant, V.M. (Eds.), *New Developments in Palynomorphic Sampling, Extraction and Analysis*. American Association of Stratigraphic Palynologists Foundation, Houston, TX, pp. 29–34.

Sowers, T., Bender, M., 1995. Climate records covering the last deglaciation. *Science* **269**, 210–214.

Spooner, I.S., Barnes, S., Baltzer, K.B., Raeside, R., Osborn, G.D., Mazzucchi, D., 2003. The impact of air mass circulation dynamics on Late Holocene paleoclimate in northwestern North America. *Quaternary International* **108**, 77–83.

Stein, J.K., 1987. Deposits for archaeologists. *Advances in Archaeological Method and Theory* **11**, 337–395.

St. Louis, M., 2021. *Summer Lake Wildlife Area Management Plan*. State Wildlife Management Assessment, Oregon Department of Fish and Wildlife, Salem. dfw.state.or.us/wildlife/management_plans/wildlife_areas/docs/2021_SLWA%20Management%20Plan_Revision%20Final%20Draft.pdf, accessed November 24, 2021.

Thomas, D.H., Davis, J.O., Grayson, D.K., Melhorn, W.N., Thomas, T., Trexler, D.T., Adovasio, J.M., *et al.*, 1983. The archaeology of Monitor Valley 2, Gatecliff Shelter. *Anthropological Papers of the American Museum of Natural History* **59**. doi.org/hdl.handle.net/2246/267.

Thompson, R.S., 1996. Pliocene and early Pleistocene environments and climates of the western Snake River Plain, Idaho. *Marine Micropaleontology* **27**, 141–156.

Vacco, D., Clark, P., Mix, A., Cheng, H., Edwards, R., 2005. A speleothem record of Younger Dryas cooling, Klamath Mountains, Oregon, USA. *Quaternary Research* **64**, 249–256.

White, W.B., 2007. Cave sediments and paleoclimate. *Journal of Cave and Karst Studies* **69**, 76–93.

Wigand, P.E., 1987. Diamond Pond, Harney County, Oregon: vegetation history and water table in the eastern Oregon desert. *Great Basin Naturalist* **47**, 427–458.

Wigand, P.E., Rhode, D., 2002. Great Basin vegetation history and aquatic systems: the last 150,000 years. In: Herschler, R., Madsen, D.B., Currey, D.R. (Eds.), *Great Basin Aquatic Systems History*. Smithsonian Institution Press, Washington, DC., pp. 309–367.

Williams-Dean, G., Bryant, V. M., 1975. Pollen analysis of human coprolites from Antelope House. *Kiva* **41**, 97–111.

Wood, J.R., Wilmshurst, J.M., 2012. Wetland soil moisture complicates the use of *Sporormiella* to trace past herbivore populations. *Journal of Quaternary Science* **27**, 254–259.

Wood, J.R., Wilmshurst, J.M., 2016. A protocol for subsampling Late Quaternary coprolites for multi-proxy analysis. *Quaternary Science Reviews* **138**, 1–5.

Wood, J.R., Wilmshurst, J.M., Wagstaff, S.J., Worthy, T.H., Rawlence, N.J., Cooper, A., 2012. High-resolution coproecology: using coprolites to reconstruct the habits and habitats of New Zealand's extinct upland moa (*Megalapteryx didinus*). *PLoS ONE* **7**, e40025.

Wriston, T., Smith, G.M., 2017. Late Pleistocene to Holocene history of Lake Warner and its prehistoric occupations, Warner Valley, Oregon (USA). *Quaternary Research* **88**, 491–513.

https://doi.org/10.1017/qua.2023.44 Published online by Cambridge University Press